Sudan University of Science and Technology

College of Graduate Studies

A Study of Radiation Dose Reduction for Patients Undergoing Abdominal Computed Tomography with Contrast Agent

دراسة تخفيض جرعة الإشعاع للمرضى الخاضعين للأشعة المقطعية للبطن باستخدام وسيط التباين

A thesis Submitted for Fulfillment of the Requirement of PhD Degree in Medical Physics

By:
Mr. Hussein Ibrahim Hussein Adam
M.Sc in Physics

Supervisor:
Prof. Dr. Abdelmoneim Adam Mohamed Sulieman

Co-Supervisor:
Prof. Dr. Abdelrahman Mohamed Elnour Fadlelmoula

2022

Sudan University of Science and Technology

College of Graduate Studies

A Study of Radiation Dose Reduction for Patients Undergoing Abdominal Computed Tomography with Contrast Agent

دراسة تخفيض جرعة الإشعاع للمرضى الخاضعين للأشعة المقطعية للبطن باستخدام وسيط التباين

A thesis Submitted for Fulfillment of the Requirement of PhD Degree in Medical Physics

By:

Mr. Hussein Ibrahim Hussein Adam

M.Sc in Physics

Supervisor:

Prof. Dr. Abdelmoneim Adam Mohamed Sulieman

Co-Supervisor

Prof. Dr. Abdelrahman Mohamed Elnour Fadlelmoula

2022

Ref: SUST/ CGS/A11

Approval Page

(To be completed after the college council approval)

Name of Candidate: | **Hussein** | **Ibrahim** | **Hussein** | **Adam** |

Thesis title: Study of Radiation Dose Reduction for patient Undergoing Abdominal Computed Tomography with Contrast Agent -

Degree Examined for: PhD. in Medical Physics'

Approved by:

1. External Examiner

Name: Nahla Omer Alanta

Signature: ..... **Date:** 11/8/2022

2. Internal Examiner

Name: Prof. Elsafi Ahmed Abdalla

Signature: ..... **Date:** 4/12/2022

3. Supervisor

Name: Abdelrahman M Elnour

Signature: ..... **Date:** .....

Dedication

To my parents,

To my wife and my children

To anyone who taught me a letter,

To all my grand family.

Acknowledgements

To the main supervisor, Professor Abdelmoneim Adam Mohamed Sulieman, whom I referred to him as a supervisor of my research, and I found him to be a guide in various aspects of life, so I learned from him brotherhood, generosity, generosity, love of teamwork and mastery in scientific publishing. This is the result of his continuous guidance throughout the completion of this research. I extend my thanks and appreciation to him.

I also extend my heartfelt thanks to His Excellency, Professor Abdul Rahman Muhammad Nour, who was honored to be the assistant supervisor of this research. He has the highest degree in the practical applications I presented in this study.

Thanks are also extended to all the workers in the radiology departments in the hospitals for their cooperation and assistance in collecting the study data.

I also would like to thank all the teaching staff who gave me their knowledge in various educational stages.

My thanks also go to the Deanship of Scientific Research at Princess Nourah bint Abdulrahman University and the Deanship of Scientific Research at Prince Sattam bin Abdulaziz University for their support in the publication of the scientific papers.

Finally, I would like to thank my parents and wife for their continued support.

Contents

List of Tables

List of Figures

List of **Abbreviations**	
AAPM	American Association of Physicists in Medicine
ACR	American College of Radiology
ADMIRE	Advanced Modeled Iterative Reconstruction
AEC	Automatic Exposure Control
AIDR3D	Adaptive Iterative Dose Reduction 3Daimentions
ALARA	As Low As Reasonably Achievable
ASIR	Adaptive Statistical Iterative Reconstruction
BMI	Body Mass Index
CAD	Coronary Artery Disease
CNR	Contrast to Noise Ratio
CT	Computed Tomography
CTDI	Computed Tomography Dose Index
CTDIvol	Computed Tomography Dose Index, Volume
CTDIw	Computed Tomography Dose Index, Weighted
CVD	Cardio-Vascular Disease
DLP	Dose Length Product
DRLs	Diagnostic Reference Levels
DSA	Digital Subtraction Angiography
EU	European Commission

FBP	Filtered Back Projection
FDA	Food and Drug Administration
HU	Hounsfield Unit
IAEA	International Atomic Energy Agency
ICRP	International Commission on Radiological Protection
IR	Iterative Reconstruction
IRIS	Iterative reconstruction in image space
MDCT	Multi Detector row Computed Tomography
MHU	Mega Heat Units
MSAD	Multiple Scan Average Doses
PMMA	Polymethyl Methacrylate Phantom
ROI	Region Of Interest
SAEC	Sudan Atomic Energy Commission
SAFIRE	Sinogram Affirmed Iterative Reconstruction
UNSCEAR	United Nations Scientific Committee on the Effects of Atomic Radiation
WHO	World Health Organization

ABSTRACT

The present study aims to estimate the patient's radiation dose during contrast-enhanced multiphase abdominal CT examinations to reduce the patient's radiation dose and radiogenic risk associated with the procedures. The study was composed of 642 adult and pediatric patients who underwent multiphase contrast-enhanced abdominal CT examinations in nine hospitals. The data were classified according to the study protocol, consisting of standard-dose protocol, Combination of low dose with standard and high-quality dose protocol, and 3D sure exposure low dose protocol. The mean ± SD and range of patient dose in terms of volume CT dose index CTDIvol (mGy) and dose length product (DLP) mGy.cm respectively for the complete procedure were 12.88 ± 2.75 mGy (3.3–28.18) and 2555.4 ± 873.57 mGy.cm (257–9263.5) for standard-dose protocol and 7.01 ± 3.05 mGy (4–15.23) and 1331.48 ± 594.64 mGy.cm (708.5–3279) for Combination of low dose with standard and high-quality dose protocol and 5.2 ± 1.55 mGy (2.6–9.78) and 811.8 ± 156.76 mGy.cm (482.7–1155.8) for pure 3D sure exposure low dose protocol. The mean and range of effective doses were 38.33 ± 22.9 mSv (4.0–138.9), 19.97 mSv (10.6–49.2), and 12.18 mSv (7.2–17.3) respectively for previously mentioned protocols. The wide range of doses indicates that some patients have received an elevated dose, especially in standard dose protocol. Predicted cancer risk per procedure were 2, 1, and 0.6 cancer case pre thousandth procedures respectively for mentioned protocols, 3D sure exposure low dose protocol provides 40 to 70 % reduction in effective dose without compromising the image quality.

المستخلص

الهدف من هذه الدراسة هو تقدير الجرعة الاشعاعية لدي المرضى خلال فحوصات الاشعة المقطعية باستخدام وسيط التباين وذلك بغرض تخفيض الجرعة الاشعائية وتخفيض مخاطر حدوث السرطانات.
اشتملت الدراسة على 642 مريض (بالغين واطفال) تعرضوا للفحص المعني في تسعة مستشفيات ، تم تقسيم المرضى وفق نظام طريقة إجراء الفحص وهو البروتوكول العام ، بروتوكول الجرعة المخفضة وبروتوكول الجرعة ذات الجودة العالية خلال مراحل الفحص المختلفة. تم تقييم الجرعة الاشعاع بحساب مؤشر الجرعة المقطعية لوحدة الحجوم CTDI vol (mGy) والجرعة للفحص DLP (mGy.cm) والجرعة المؤثرة E (mSv) فوجدت 12.88 ± 2.75 mGy (3.3 الى 28.18) و mGy.cm 2555.4 ± 873.57 (257 الى 9263.5) وmSv 38.33 ± 22.9 (4.0 الى 138.9) ، و ± 7.01 3.05 mGy (4 الى 15.23) و mGy.cm 1331.48 ± 594.64 (708.5 الى 3279) و 19.97 mSv (10.6 الى 49.2)، وmGy 5.2± 1.55 (2.6 الى 9.78) و mGy.cm 811.8 ± 156.76 (482.7 الى 1155.8) و mSv 12.18 (7.2 الى 17.3) على التوالي لكل من فحص جميع المراص بنظام الجرعة الاساسي ، والفحص بنظام الجمع بين الجرعة المخفضة والجرعة الاساسي او الجرعة ذات الجودة العالية، والفحص بالجرعة المخفضة لجميع المراحل. الفروقات الواضحة في الجرعات الاشعائية بين ادنى واعلى جرعة تشير الى تعرض المرضى لجرعات زائدة عن الحوجة ، خاصة في الفحص بالنظام الاساسي لجميع مراحل الفحص . خطر الاصابة بالسرطان نتيجة لهذه الفحوصات كانت تقريبا اثنين لكل 1000 فحص ، و واحد لكل 1000 فحص ، و واحد لكل 2000 فحص على التوالي لكل من فحص جميع المراص بنظام الجرعة الاساسي ، والفحص بنظام الجمع بين الجرعة المخفضة والجرعة الاساسي او الجرعة ذات الجودة العالية ، والفحص بالجرعة المخفضة لجميع المراحل. وهذه الاخيرة انخفضت الجرعة المؤثرة بنسبة تتراوح بين 40% الى 70% مقارنة بالطرق الاخرى المذكورة دون التأثير على جودة الصورة.

CHAPTER ONE

INTRODUCTION

CHAPTER ONE

INTRODUCTION

1.1 Introduction:

The challenge of patient protection from exposure to ionizing radiation in medical imaging has been increased after the advancement of multi-detector computed tomography (MDCT). Advanced technology CT systems (not least, multi detector CT and helical acquisition) have enabled short CT scanning time, reduced amounts of contrast medium and volumetric acquisition, all moving towards more accurate diagnostic capability. Annually around 400 million CT examination performed in the world wide, the average frequency of CT examination per year for every 1000 population is about 55 CT examination (UNSCEAR,2022). The percentage of increasing in number of CT examination in united state since 1980 to 1998 is about 900% (Nickoloff et al, 2001). CT examination contributes in overall medical radiation exposure by up to 75% while it is frequency is just about 11% compared with other imaging procedures (Fazel et al., 2009). Recently, the overall contribution of CT examinations in the annual collective effective dose is about 62% with frequency of just around 10% compared with other medical imaging procedures. The contribution of Sudan in the total frequency of the global number of CT examinations is about 1% with 16% of dose contribution to the global population (UNSCEAR, 2022). Today, CT is a prominent source of exposure to ionizing radiation as results of continues emerging of wide range of new clinical applications and the feasibility of conducting multi-phase enhancement CT studies, such as CT angiography and CT Urography. Vascular CT in particular represents one of the main sources of elevated radiation exposure compared to other CT examinations due to the large area covered and the potential numbers of procedures patient might go through. The effective doses from diagnostic CT procedures are

typically estimated to be in the range of 1 to 10 mSv, this range is not much less than the lowest dose of 5 to 20 mSv received by some of the Japanese survivors of the atomic bombs, those survivors who are estimated to have experienced doses only slightly larger than those encountered in CT have demonstrated small but increased radiation-related excess relative risk for cancer mortality (FDA, 2017). The probability of absorbed dose to induce cancer or heritable mutations leading to genetically associated disease in offspring is thought to be very small for radiation doses of the magnitude that are associated with CT procedures. Such estimates of cancer and genetically heritable risk from x-ray exposure have a broad range of statistical uncertainty and there is some scientific controversy regarding the effects from very low doses and dose rates (Feinendegen & Cuttler 2018). The manufacturers of CT-equipment have an important role in decreasing radiation dose; each modern manufacturer is conscious of the problem with high radiation doses and has developed automatic exposure control techniques and vendor low dose technique by reemerging iterative reconstruction technique. However, there is still much work to do, both by users and producers concerning defining the acceptable reference image quality for different diagnostic subjects (Lieberman, Huda et al. 2002). In addition, rapidly growing use of pediatric CT and the potential for increased radiation exposure to children undergoing these scans remain a public health concerns, a special considerations should be applied when using pediatric CT (FDA, 2017). Doses from a single pediatric CT scan have a range from about 5 mSv to 60 mSv among children who have undergone CT scans approximately one-third had at least three scans.

Radiation dose from CT procedures are varies from patient to patient. A particular radiation dose will depend on the size of the body part examined, the type of procedure and the type of CT equipment and its operation. The ease of acquiring images sometimes results in unnecessary exposure of patients to

radiation, particularly in developed countries. However, no comprehensive data is available to permit estimation of the extent of this practice and reducing the dose can have an adverse impact on the image quality produced. Such reduced image quality may be acceptable in certain imaging applications.

1.2 Problem of the Study:

With highlighting the contribution of Sudan to the global population dose and the consideration of protecting patient from radiogenic risk associated with exposure to ionizing radiation in medical imaging, especially in computed tomography examination (CT scan), which it classified as the prominent source of elevated radiation dose in medical imaging. As results of ease accessibility of CT in Khartoum state (Sudan), a large number of contrast enhanced multi-phase CT examination performed. In abdominal CT with a contrast agent, patients receives higher radiation dose than other CT examination, because patients may exposed to the radiation more than once (before, during, and after enhancing contrast agent) according to imaging modalities, body part examined, and local protocol used. There are many different variations in patient dose from hospital to another hospital also the variation may be found in the same hospital or from modality to another; these variations may be attributed to variation in scan length, un accurate adjustment of scan field, bad practice coming from lack of training in manipulation of CT exposure parameters, excessive number of scanning phases to compensate the diagnostic task, un familiar in use dose saving technique. All these bad practice leads to higher effective doses. Therefore, it is essential to ensure that technology is optimized to deliver patient-specific radiation dose conforms to ALARA principles as low as reasonably achievable (Valentin et al. 2007).

1.3 Objectives of the Study:

1.3.1 General objective:

The general objective of this study is to reduce the radiation dose for patients undergoing abdominal CT examination with contrast agent without compromising the diagnostic image quality.

1.3.2 Specific objectives:

The specific objectives of this study are:

1) To evaluate the radiation dose for patients during a multi-phase abdominal CT examination with contrast agent.
2) To estimate the effective dose and radiation risks of the procedures.
3) To adjust the imaging parameters to optimize patient's radiation dose.
4) To establish diagnostic reference level for contrast enhanced multi-phase abdomen CT examinations.

1.4 Thesis Outline:

This thesis is concerned with assessing the patient's radiation dose during abdominal contrast-enhanced CT examination In order to optimize radiation dose and establish diagnostic reference level for the concerned procedures.

A thesis is divided into the following chapters:

Chapter one: contains the introduction to thesis, scope of the study problem and thesis outcome.

Chapter two: contains the theoretical background of the thesis, specifically, it reviews the dose for absorbed dose measurements and calculations. This chapter also includes a summary of previous works performed in this field.

Chapter three: describes the materials and methods used to measure dose for CT machines and explains in detail the methods for calculating and optimizing the dose.

Chapter four: presents the results and interpretation of row data collected from different hospitals.

Finally, chapter five: present the discussion, conclusion, thesis recommendations, and suggestions for future work.

1.5 Thesis outcome:

This study contributes directly to reducing radiation dose for patients undergoing abdominal CT examinations with contrast agent through the application of the low dose protocol, which is positively reflected in reducing the expected risks of cancer incidence occurs from exposure to ionizing radiation, and this study also contributes to enriching the scientific library through published articles listed below.

1.6 Publications:

A. Published Articles

1. Sulieman,A., **H. Adam,** N. Tamam, M. Alkhorayef, A. Alhailiy, S. Alghamdi, A. Elnour, O. Alomair, Y. Alashban, M.U. Khandaker, D.A. Bradley. A survey of the pediatric radiation doses during multiphase abdominal computed tomography examinations. *Radiation Physics and Chemistry*. Volume 188, 2021, page 1-6. Impact Factor 2.858, ranking it 3 out of 34 in Nuclear Science & Technology.

2. Sulieman, A.,**Adam**, H., Elnour, A., Tamam, N., Alhaili, A., Alkhorayef, M., Alghamdi, S., Khandaker, M.U., Bradley, D.A. Patient radiation dose reduction using a commercial iterative reconstruction technique package. *Radiation Physics and Chemistry* Volume 178, January 2021, Article number 108996. Page 1-6. Impact Factor 2.858, ranking it 3 out of 34 in Nuclear Science & Technology.

3. Sulieman, A., **Adam, H.**, Mahmoud, M.Z., Hamid, O., Alkhorayef, M., Bradley, D.A. Radiogenic risk assessment for abdominal vascular computed tomography angiography. *Radiation Physics and Chemistry*.

Volume 168, March 2020, Article number 108523. Page 1-5. Impact Factor 2.858, ranking it 3 out of 34 in Nuclear Science & Technology.

B. Submitted articles:

4. Rasha Jaafar., Abdelrahman Elnour., **H.Adam**., Abdelmoneim Sulieman., Nissren Tamam., Abdullah Almujally., Nouf H. Abuhadi., Mayeen Uddin Khandaker.,D.A. Bradley., Estimation of Organ and Effective Doses in Vascular lower extremity Computed Tomography Angiography. *Applied Radiation and Isotopes*. Impact Factor of this journal is 1.513, ranking it 15 out of 34 in *Nuclear Science & Technology*

5. **H. Adam,** A. Elnour, A. Sulieman. Estimation the effective dose and cancer risk for patients underwent high resolution chest CT examination for screening COVID-19. *Radiation Physics and Chemistry* Impact Factor 2.858, ranking it 3 out of 34 in Nuclear Science & Technology.

C. Conference Presentation :

1. **H. Adam**, A. Elnour, A. Sulieman. Estimation the effective dose and cancer risk for patients underwent high resolution chest CT examination for screening COVID-19. The 4th International Forum on Advances in Radiation Physics (IFARP-4), 27 – 31 March 2022, Riyadh – Saudi Arabia.

CHAPTER TWO

THEORETICAL BACKGROUND and LITERATURE REVIEW

CHAPTER TWO

THEORETICAL BACKGROUND and LITERATURE REVIEW

2.1 Theoretical backgrounds:

This section present science based background related to imaging theory, radiation quantity and units, development of CT facilities, radiation dose optimization and image quality analysis.

2.1.1 Introduction to X-ray:

An X-ray is a form of high-energy electromagnetic radiation that can cause ionization when it penetrates a human body. Most X-rays have a wavelength ranging from 0.03 to 3 nanometers, corresponding to frequencies in the range 30 petahertz to 30 exahertz (3×1016 Hz to 3×1019 Hz) and energies in the range 100 eV to 200 keV. (Fig 2.1) X-ray wavelengths are shorter than UV rays and typically longer than those of gamma rays. In many languages, X-radiation is referred to as Röntgen radiation, after the German scientist Wilhelm Röntgen, who discovered it on November 8,1895.

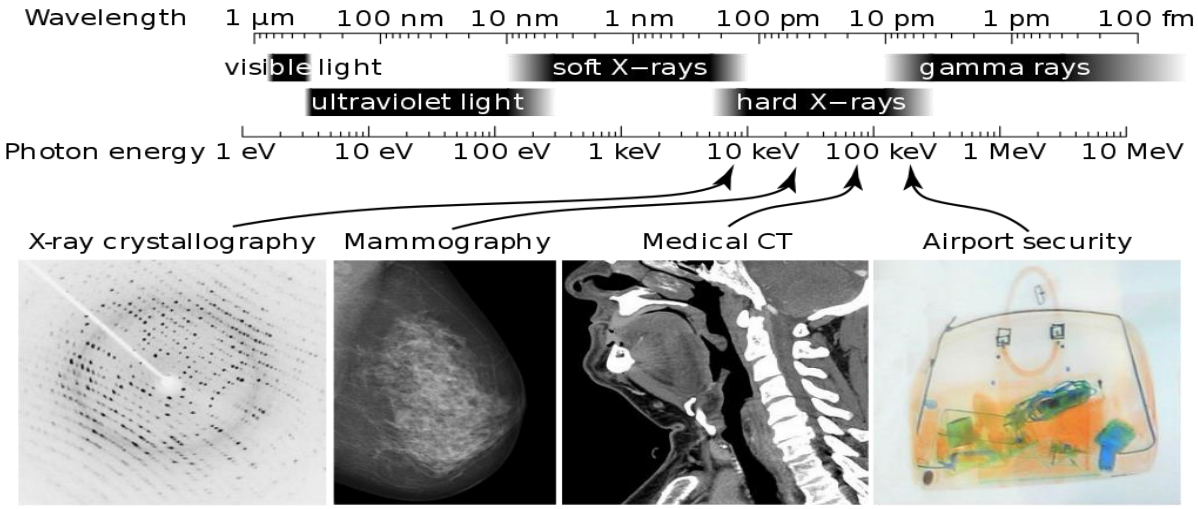

Fig: 2.1 show different applications use different parts of the X-ray spectrum (en.wikipedia.org/wiki/X-ray)

2.1.2 Radiation quantities and units:

Accurate measurement of radiation is very important in any medical use of radiation, be it for diagnosis or treatment of disease. Several quantities and units were introduced for the purpose of quantifying radiation and the most important of these are Exposure, Dose, Equivalent dose and Activity (Podgoršak 2006).

- Exposure is related to the ability of photons to ionize air. Its unit roentgen (R) is defined as charge of $2.58 \times 10{-}4$ C produced per kg of air.
- Dose (absorbed dose) is defined as the energy absorbed per unit mass of medium. Its unit gray (Gy) is defined as 1 J of energy absorbed per kg of medium.
- Equivalent dose (effective dose) is defined as the dose multiplied by a radiation-weighting factor. The unit of equivalent dose is sievert (Sv).
- Activity of a radioactive substance is defined as the number of decays per-time. Its unit is Becquerel (Bq) corresponding to one decay per second.

One of the most important characteristics of interaction of radiation beams with matter is the dose deposition in water, radiation physics and more ever medical physics depends on the properties dose deposition in tissue for both the diagnosis of disease with radiation (imaging physics) as well as the radiation oncology physics is the treatment of disease with radiation (Podgoršak 2006). Organ absorbed doses and effective doses can be used for comparing radiation exposure among different medical imaging procedures, as well as comparing alternative imaging options, and it is helpful guide for dose optimization efforts (Fig: 2.2) Individual dose estimations are very important for relatively radiosensitive patient populations such as children and for radiosensitive organs such as the eye lens (Quinn, Gao et al. 2020).

2.1.3 CT machine components:

Computed tomography (CT) is medical imaging equipment designed for production of cross-sectional images using x-rays and computers. Fig (2.3), the major advantages of CT over conventional x-ray technique is the superiority of differentiating soft tissues (Hathcock and Stickle 1993). The term “computed tomography”, or CT, refers to a computerized x-ray imaging procedure in which a narrow beam of x-rays is aimed at a patient and quickly rotated around the body, producing signals that are processed by the machine’s computer to generate cross-sectional images or “slices” of the body. These slices are called topographic images and contain more detailed information than conventional x-rays. Once a number of successive slices are collected by the machine’s computer, they can be digitally “stacked” together to form a three-dimensional image of the patient that allows for easier identification and location of basic structures as well as possible tumors or abnormalities (NIH, 2019).

2.1.4 CT history and development:

The English engineer G.N. Hounsfield was built it is first commercial medical X-ray computed tomography (CT) scanner for the company EMI Ltd In 1972. The scanner composed of X-ray tube and two detector elements moving incrementally around the patient as a pure head scanner. It was able to acquire twelve slices with 13 mm slice thickness each and reconstruct the images with a matrix of 80 × 80 pixels in approximately 35 min. By then the acquisition time for one image decreased from 300 s in 1972 to 1–2 s, thin slices of down to 1 mm became possible and the in-plane resolution increased from 3 line pairs per cm (lp/cm) to15 lp/cm with typically 5122 matrices (Ulzheimer, Bongers et al. 2018).

The technical development in CT equipment, including the development of slip

rings, increased X-ray tube heat capacity, advances in detector technology and improvement in computers now permit rapid sub-second exposures for acquiring sub-millimeter sections and almost instantaneous image reconstruction. These improvements have brought benefits in clinical examination, extending the applications of CT into new areas and facilitating difficult or demanding examinations in all applications (Tack, Gevenois et al. 2007). Today computed tomography represents a perfectly natural and established technology that has become an indispensable and integral component of routine work in clinics and medical practices (Siemens 2011).

The invention of computed tomography is considered to be the most significant innovation in the field of radiology since the discovery of X-rays. This cross-sectional imaging technique provided diagnostic radiology with better insight into the pathogenesis of the body, thereby increasing the chances of recovery. In 1979, G.N. Hounsfield and A.M. Cormack were awarded the Nobel Prize in medicine for the invention of CT (Siemens 2011).

Multidetector row computed tomography (MDCT) has modified the imaging approach for the assessment of many diseases such as screening of colorectal polyps, the detection of lung nodules, the screening for cardiac and coronary artery diseases and the easy three-dimensional rendering of various vessels in any part of the body (Marchal, Vogl et al. 2005). Advantages of the technique include the rapid acquisition and three-dimensional rendering of images even of the pulsating heart or vessels. The spatial resolution is improving and so is the diagnostic confidence. Due to the faster acquisition time, we are moving towards automated procedures of acquisition and image reading (Marchal, Vogl et al. 2005). The acquisition times of mechanical CT scanners were expected to be far too long for high quality cardiac imaging for the next years or even decades to come, a completely new technical concept for a CT scanner without

moving parts for extremely fast data acquisition within 50 ms was suggested and promoted as cardiovascular CT (CVCT) scanner. These scanners were also called “Ultrafast CT” scanners or “Electron Beam CT” (EBT or EBCT) scanners. High cost and limited image quality combined with low volume coverage prevented the wide propagation of the modality. Larger volume coverage in shorter scan times and improved through-plane resolution became feasible after the broad introduction of 4-slice CT systems by all major CT manufacturers in 1998 (Ulzheimer, Bongers et al. 2018). Three technological developments of CT scanners require: specific slip-ring gantry designs, very high power x-ray tubes, and interpolation algorithms to handle the non-coplanar projection data. Thus, modern CT scanners now offer flexible unlimited clinical tools (Tack, Gevenois et al. 2007). In 2007, one vendor introduced a MDCT system with 128 simultaneously acquired slices, based on a 64-row detector with 0.6 mm collimated slice width (38.4 mm z-axis coverage) and double z-sampling by means of a z-flying focal spot. Later, simultaneous acquisition of 256 slices became available with a CT system equipped with a 128-row detector (0.625 mm collimated slice width, 80 mm z-axis coverage) and double z-sampling (Ulzheimer, Bongers et al. 2018).

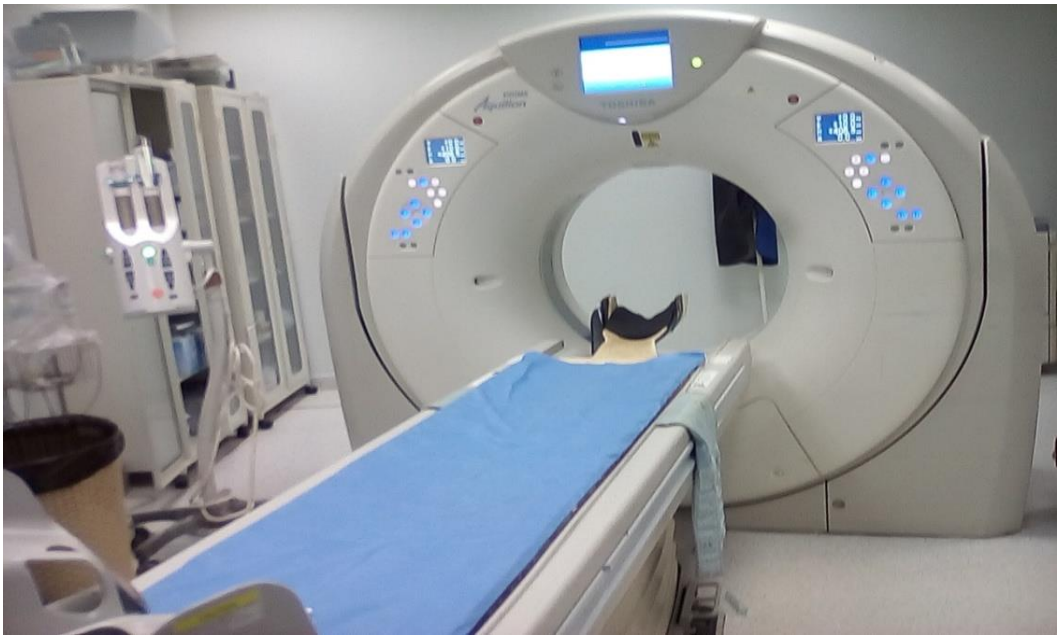

Fig: 2.2 show Toshiba aquiline prime 128 slice CT machine equipped in diagnostic center C.

2.1.5 X-Ray tube and generator:

In state of the art, X-ray tube/generator combinations provide a peak power of 60 – 120 kW, usually at various user-selectable voltages, e.g., 70 –140 kV in steps of 10 kV. In a conventional tube design, an anode plate of typically 160 – 220 mm diameter rotates in a vacuum housing (Fig: 2.4). The heat storage capacity of anode plate and tube housing—measured in Mega Heat Units (MHU)—determines the performance level: the bigger the anode plate is, the larger is the heat storage capacity, and the more scan-seconds can be delivered until the anode plate reaches its temperature limit. The anode plate constitutes an outer wall of the rotating tube housing; it is therefore in direct contact with the cooling oil and can be efficiently cooled via thermal conduction. This way, a very high heat dissipation rate and fast anode cooling is achieved, enabling high power scans in rapid succession. Due to the central rotating cathode, permanent electromagnetic deflection of the electron beam is needed to position and shape the focal spot on the anode (Ulzheimer, Bongers et al. 2018). Recent progress in X-ray tube design has led to the introduction of X-ray tubes capable of providing high power reserves at 70, 80 and 90 kV. They have the potential to

enable contrast-enhanced low kV scans in adult and in obese patients without compromising CNR (Ulzheimer, Bongers et al. 2018).

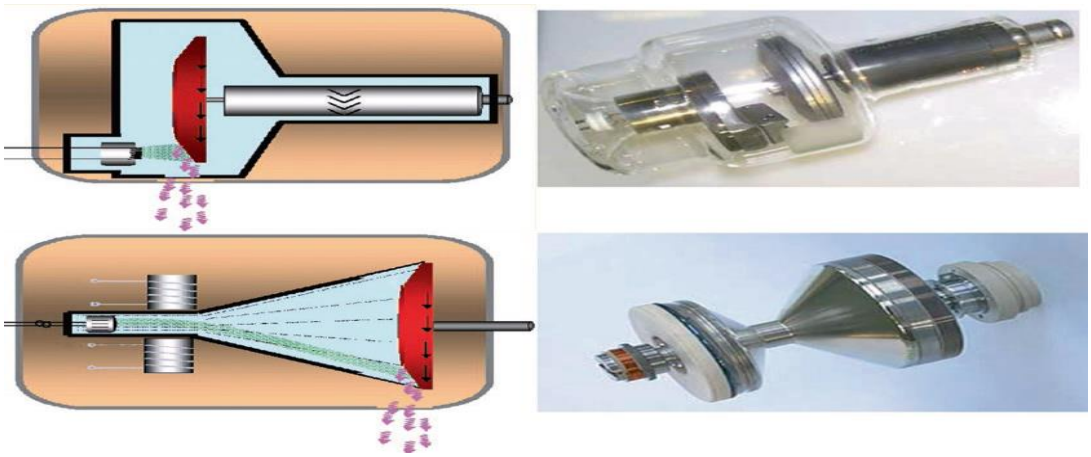

Fig (2.3) : show different tube generator (Ulzheimer, Bongers et al. 2018).

2.1.6 Iterative reconstruction method:

As an increasing use of CT in medical field, especially in radiation-sensitive populations (children, young adults, and pregnant female patients), radiation dose reduction tools has been in continuously developing by CT manufacturers (Raman, Johnson et al. 2013). Although all the major CT manufacturers offer significant tools to reduce radiation dose (Raman, Johnson et al. 2013). Recently, Iterative reconstruction (IR) methods were re-emerged in clinical transmission x-ray computed tomography (CT) due to it is higher computational demands in comparison with analytical methods (Beister, Kolditz et al. 2012). Therefore, all major vendors of clinical CT systems were used IR method to enhance the efforts for ALARA principles (as low as reasonably achievable). There are two major benefits of applying IR techniques in Medical imaging CT scanners; those are noise reduction and artifact reduction, with noise reduction being of key interest since it allows for lower dose imaging (Willemink, de Jong et al. 2013). There is a variety of different iterative reconstruction techniques commercially available, such as ASIR, VEO and ASIR-V (GE Healthcare, USA), IRIS, SAFIRE and ADMIRE (Siemens Healthcare, Germany), iDose

(Philips, the Netherlands) and AIDR3D (Toshiba). The technical realization is highly vendor specific, applying some or all of the steps described above, often in a simplified realization to achieve acceptable image reconstruction times in a routine clinical environment. All approaches aim at reducing image noise without degrading spatial resolution and without significantly altering the well-established image appearance and noise structure of a filtered back-projection reconstruction (Ulzheimer, Bongers et al. 2018). To get full advantage of IR, Siemens was introduced Sinogram Affirmed Iterative Reconstruction—SAFIRE in 2010, SAFIRE is an advanced IR technique that utilizes both projection space (raw) data and image space data, with the number of iterations in each "space" dependent on the needs of a specific scan. In contrast to other pure raw-data-based IR algorithms, SAFIRE is available right on the scanner and can reconstruct up to 20 images per second. Therefore, SAFIRE can easily be used in routine clinical workflow, with well-established reconstruction kernels, providing up to 60% reduction in dose. SAFIRE is not for dose reduction alone; it can also be used to improve image quality, as in the case of very low dose pediatric imaging, or to reduce noise in obese patient scans. SAFIRE strengths 1–5 can be previewed for each reconstruction, with the default strength set at 3 The level of noise reduction and noise texture will change depending on the strength that the user chooses for each reconstruction, with strength 1 being noisier and strength 5 being smoother (Raupach 2012).

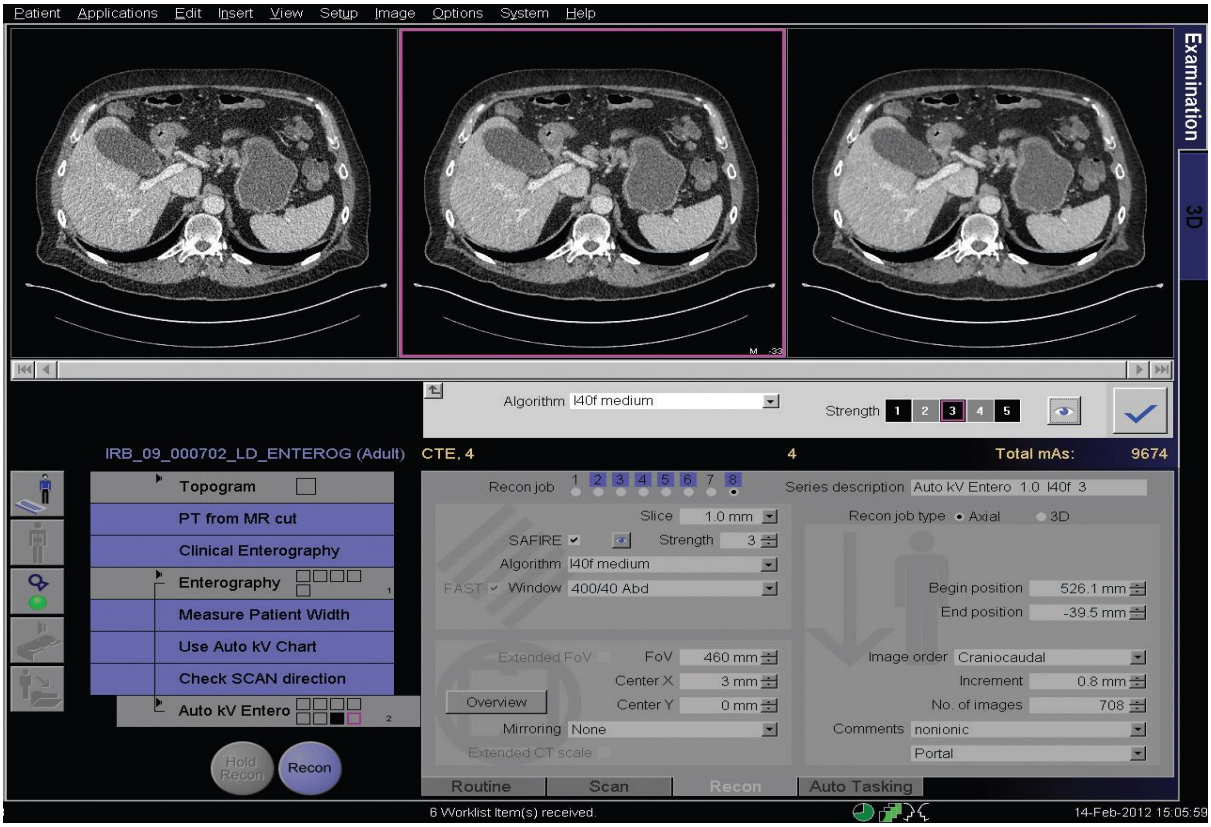

Fig (2.4) SAFIRE interface Preview of SAFIRE strength settings 1, 3 & 5 with an I40 kernel typical of routine abdomen exam (Raupach 2012).

The most recent algorithm for noise reduction is the Adaptive Iterative Dose Reduction 3D (abbreviated as AIDR 3D). AIDR 3D is specially designed to work iteratively in both three dimensional reconstruction data and raw data domains (Geleijns and Irwan 2012). AIDR 3D have an important component contributing to dose reduction, sure exposure tube current modulation tailors tube current to account for differences in patient size and shape within different regions of the body.(Fig 2.6) In addition, sure exposure adjusts the tube current appropriately for the selected acquisition and reconstruction parameters. Sure exposure tube current modulation has the ability to reduce patient dose while maintaining optimized image quality. Therefore, sure exposure automatically adjust the tube current in CT imaging to account for size of the patient and thus provides greater consistency of image quality between patients as well as manual adjustment of acquisition parameters to account for patient size provides

inconsistent image quality between patients. In the same way that AEC offers automated patient size adjustment in planar x-ray imaging (Van der Molen, Joemai et al. 2012). The best image quality in diagnostic radiology is the acceptable image to answer our clinical question after applying LARA principles. Individual patients undergoing CT imaging have different needs depending on their size and shape and depending on their diagnostic task. Thus, it is essential that tools to be used to tailor each scan for the individual patient to obtain an excellent image quality while maintaining the lowest possible radiation dose (Van der Molen, Joemai et al. 2012). Analogous to Automatic Exposure Control (AEC) in x-ray imaging, the increased utilization in CT has led to the invention of new technologies such as sure exposure for managing dose on patient specific basis (Geleijns and Irwan 2012). Sure exposure low dose is a sophisticated suite of dose reduction techniques applying integration of acquisition and reconstruction parameters with advanced dose reduction algorithms (Van der Molen, Joemai et al. 2012). The collective AIDR 3D process results in strong noise reduction. The ultimate goal of CT technology is to create the best diagnostic image quality while minimizing radiation dose to the patient. Individual patients undergoing CT imaging have different needs depending on their size and shape and depending on the diagnostic task. Therefore, the pest image quality of lowest radiation dose for answering diagnostic task can be obtained by tailoring these tools for each scan according to individual patient (Geleijns and Irwan 2012). These dose reduction tools have not taken in to daily practice of many centers because of lack familiarity and understanding of how these tools work (Raman, Johnson et al. 2013). However, these tools are now built into scanner software with relatively simple, intuitive interfaces and little or no day-to-day manipulation of the scanner's settings by technologists or radiologists is required (Raman, Johnson et al. 2013).

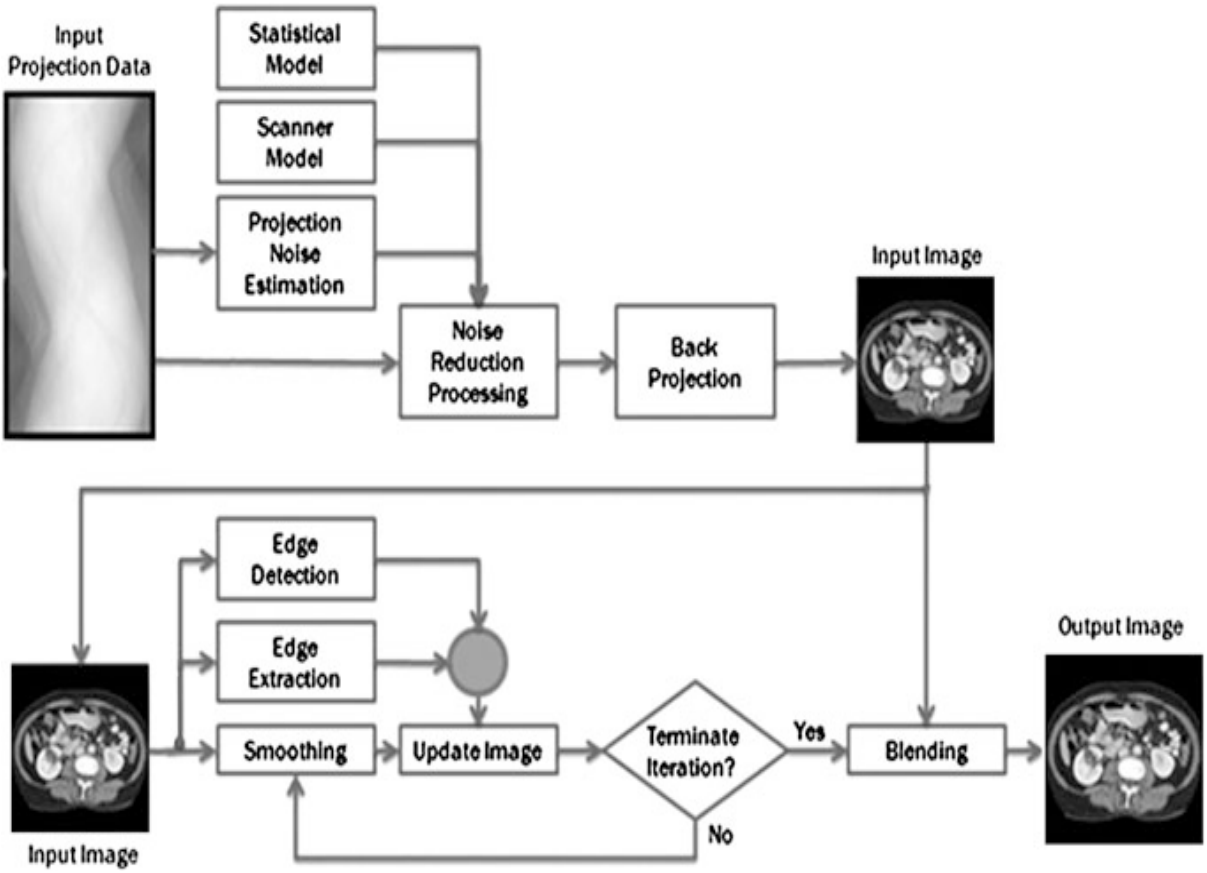

Fig (2.5) show AIDR 3D is an advanced iterative reconstruction algorithm that reduces noise in the raw data domain and also in the reconstruction process in three-dimensions (Geleijns and Irwan 2012).

2.1.7 Computed tomography parameters:

X-ray radiation dose measurement is simply a measure of the amount of energy transferred per unit mass during the interaction (Jiang 2009). The term x-ray exposure describes only the amount of ionization, not the amount of energy absorbed by the tissues being irradiated, the term “absorbed radiation dose” (also known as the radiation dose) indicates the amount of energy absorbed per unit mass (Jiang 2009). The International Commission on Radiological Protection (ICRP) recommends that dose be measured in grays (Gy):

$$1\ \text{Gy} = 1\ \text{J/kg}.$$

When multiple scans are performed in the adjacent region, x-ray dose from nearby scans also contributes to the dose to the current location, due to the long tails of the dose profile. If we combine the x-ray dose from all scans, we obtain a composite dose profile (Jiang 2009). Most CT applications involve multiple adjacent slices; dose is usually calculated from multiple scans (fig 2.7) Measurements are made at the center of the slice and several points around the periphery with plastic phantoms. This procedure accounts for the effect of scatter from the tails of each slice into the neighboring slices. Again, total dose is the central slice radiation dose, plus the scatter overlap (or tails). This is called the multiple scan average doses (MSAD). The MSAD will increase if slices overlap and decrease if there are gaps between slices, the dose at the center section is significantly higher than the single-slice dose profile (Jiang 2009).

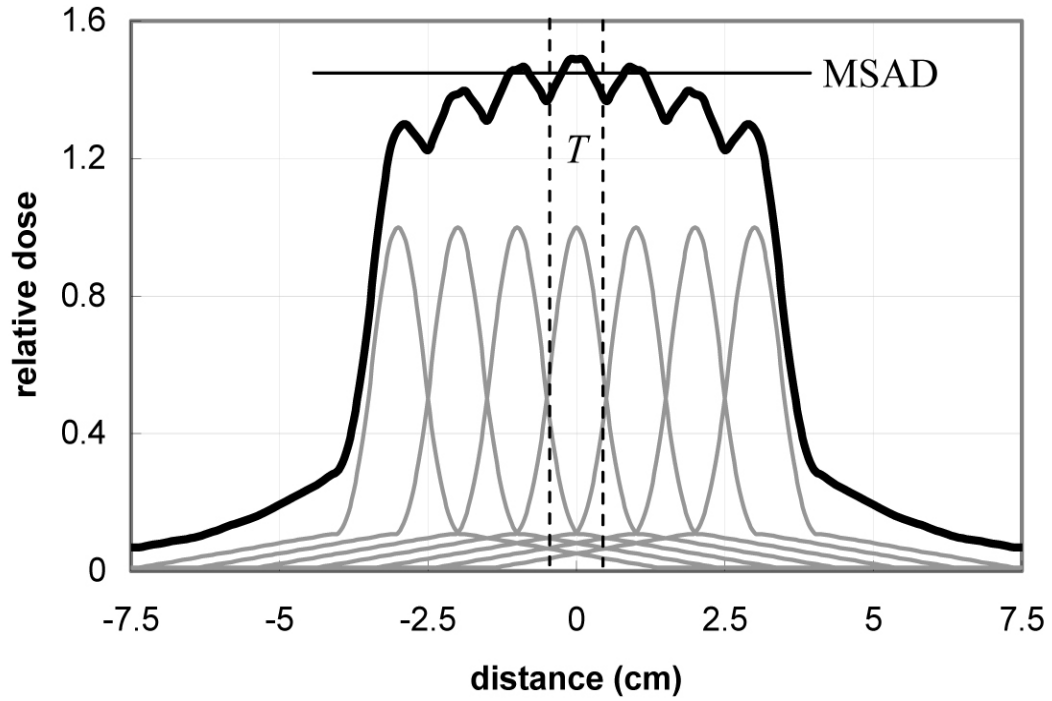

Fig (2.6) : Illustration of multiple-scan dose contributions. Multiple-scan average dose (MSAD) is obtained by summing dose contributions from adjacent slices. The figure shows

seven scans with 10-mm slice thickness at 10-mm increments (Jiang 2009).

2.1.7.1 Computed tomography dose index:

The fundamental CT dose descriptor is CTDI [unit: milligray (mGy)] which is derived from dose distribution along line of Z-axis in a single rotation of the X-ray source around it is gentry (Tack, Gevenois et al. 2007). The CTDI is what manufacturers report to the U.S. Food and Drug Administration (FDA) and prospective customers regarding the doses typically delivered for their machines. The CTDI can only be calculated if slices are contiguous, that is, there are no overlapping or gapped slices. If there is slice overlap or gaps, the CTDI is multiplied by the ratio of slice thickness to slice increment. This would technically be the MSAD, because the CTDI conditions would no longer exist. Equipment manufacturers report CTDI doses for typical head and body imaging techniques. These are equivalent to the dose a patient receives if multiple adjacent slices are acquired; Medical physicists usually use a special dosimeter called a pencil ionization chamber to measure the CTDI. This 100-mm-long thin cylindrical device is long enough to span the width of 14 contiguous 7-mm CT slices. This provides a better estimate of MSAD for thin slices than that of the single slice method. When this method is used it is referred to as the $CTDI_{100}$ (Romans 2011).

$$CTDI = \text{……..(1)}$$

Where N is the number of slices per rotation, h is the nominal slice thickness and D(z) represents the radiation dose profile along the z-axis.

The dose for body scans are not uniform across the scan field of view, the dose at the periphery of the slice is higher than the central dose. The definition of CTDIw considers only the x-ray exposure for a step-and shoot scan, and does not take into account the x-ray dose received when a helical scan is performed (Jiang 2009). The $CTDI_w$ adjusts for this by providing a weighted average of measurements at center and the peripheral slice locations (i.e., the x and y

dimensions of the slice) (Romans 2011). $CTDI_w$ is the average dose in a slice of the PMMA phantom at different positions.

……(2)

Another radiation dose parameter takes the process further step is CTDIvol, by taking account the exposure variation in the z-direction. For helical sequences the CTDIvol is obtained as:

……..(3)

This value is expressed in mGy and is displayed on most of the CT console during the scan prescription and it is now the preferred expression of radiation dose in CT dosimetry. CTDIvol is a more useful tool for comparing radiation doses among different protocols. The CTDIvol is a measure of exposure per slice and is independent of scan length. However, the scan range in z- direction can vary significantly depending on the clinical indications (Jiang 2009).

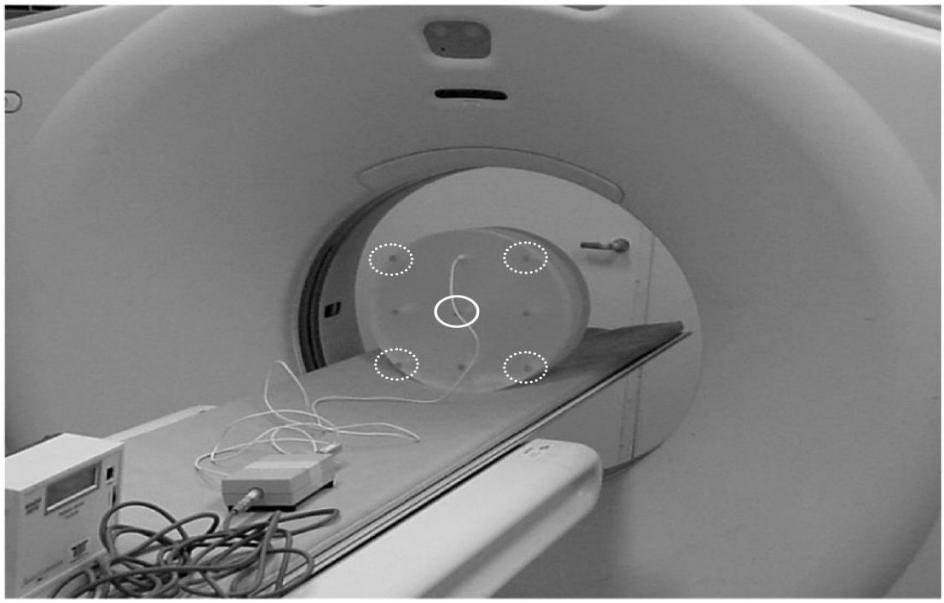

Fig (2.7) : Dose measurement setup with CTDI body phantom (32-cm diameter) and ion chamber (100-mm length) (Jiang 2009).

2.1.7.2 Dose length product:

The Dose Length Product (DLP) is the mean absorbed dose for the whole

scanned volume. To account for the integrated dose for the entire CT exam, a dose-length product (DLP) was established with the unit in mGy.cm (Jiang 2009).

$$DLP = \ . \text{scan length} \ldots\ldots\ldots\ldots\ldots\ldots\ldots (4)$$

2.1.8 Effective dose:

Effective dose [Sv] reflects the biological effects from radiation, effective dose is calculated from information about dose to individual organs and the relative radiation risk assigned to each organ. Monte Carlo simulation is often used to determine specific organ doses by simulating the absorption and scattering of x-ray photons in various tissues using a mathematical model of the human body. In a clinical environment, however, such calculation is too time consuming and not practical. Instead, a reasonable approximation of the effective dose is obtained using the equation (Jiang 2009).

$$\text{Effective dose} = k \ .DLP \ \ldots\ldots\ldots\ldots\ldots\ldots\ldots (5)$$

2.1.9 CT radiation dose:

CT involves much higher doses of radiation when it compared with plan-film radiography, a conventional anterior–posterior abdominal x-ray examination results in a dose to the stomach of approximately 0.25 mGy, which is at least 50 times smaller than the corresponding stomach dose from an abdominal CT scan (Brenner and Hall 2007). The number of CT machines and hence the examinations has increased in last decade (Pearce, Salotti et al. 2012). Due to development of powerful CT machines, new clinical applications are continue to emerge in medical fields (Elnour, Yousef et al. 2015), resulting in a marked increase in radiation exposure in the population (Brenner and Hall 2007). Radiation dose from CT procedures are varies from patient to patient. A particular radiation dose will depend on the size of the body part examined, the type of procedure, and the type of CT equipment and its operation. Typical

values cited for radiation dose should be considered as estimates that cannot be precisely associated with any individual patient, examination, or type of CT system. The actual dose from a procedure could be two or three times larger or smaller than the estimates. Facilities performing "screening" procedures may adjust the radiation dose used to levels less (by factors such as 1/2 to 1/5 for so called "low dose CT scans") than those typically used for diagnostic CT procedures. However, no comprehensive data is available to permit estimation of the extent of this practice and reducing the dose can have an adverse impact on the image quality produced. Such reduced image quality may be acceptable in certain imaging applications.

2.1.10 Biological effects and cancer risk:

Risks related to radiation exposure can be divided into two main categories: deterministic effects and stochastic effects. Deterministic effects are due to cell death and are quantified in terms of the radiation dose to a particular region. Ionizing radiation is capable of cell killing by apoptosis or radiation-induced reproductive failure, which can lead to changes in the genes involved in cell growth regulation, loss of normal nuclear structure, degradation of DNA, and tumorigenesis (Shah et al., 2012). These effects include cancer and hereditary effects, which increase an individual's lifetime risk of developing cancer or a hereditary effect in future generations. These effects have a threshold level and are not expected to be seen after a CT examination, because radiation doses do not typically reach the threshold level (Goldman 2007). The major risks are due to stochastic effects, where the probability of incidence depends on amount of absorbed dose. Stochastic effects may result in cancer and genetic effects in the offspring of the irradiated person (Verdun, Gutierrez et al. 2007). Tissue reaction effects have precise radiation dose thresholds which induce radiation risks in relatively high doses (ICRP, 2007a). The International Commission on

Radiation Protection (ICRP) adjusted nominal radiation detriment coefficients for cancer and hereditary effects as follows: 5.5*10-2 Sv and 0.2*10−2Sv-1for the whole population (ICRP, 2007a). In addition to these effects, radiation exposure has an association with certain diseases (non-cancer effect), such as respiratory diseases, stroke, heart diseases, and digestive disorders (Brenner and Hall, 2007; ICRP, 2007a). Although, radiation risks of non-cancer diseases at low doses remain uncertain, patient radiation doses must be kept at a minimum value to ensure maximum patient protection (ICRP, 2007a; Shah et al., 2012). The manufacturers of the CT-equipment have an important role in decreasing the radiation doses. Each modern manufacturer is conscious of the problem with high radiation doses and has developed automatic exposure control techniques. However, there is still much work to do, both by users and producers concerning defining the acceptable reference image quality for different diagnostic subjects (Lieberman, Huda et al. 2002). The effective doses from diagnostic CT procedures are typically estimated to be in the range of 1 to 10 mSv. This range is not much less than the lowest doses of 5 to 20 mSv received by some of the Japanese survivors of the atomic bombs. These survivors, who are estimated to have experienced doses only slightly larger than those encountered in CT, have demonstrated a small but increased radiation-related excess relative risk for cancer mortality (FDA, 2017). The probability for absorbed x rays to induce cancer or heritable mutations leading to genetically associated diseases in offspring is thought to be very small for radiation doses of the magnitude that are associated with CT procedures. Such estimates of cancer and genetically heritable risk from x-ray exposure have a broad range of statistical uncertainty, and there is some scientific controversy regarding the effects from very low doses and dose rates (Feinendegen and Cuttler 2018). There are significant increases in the probability of inducing cancer risk in multiple CT examinations. The direct evidence from epidemiologic studies is

the organ doses corresponding to a common CT study (two or three scans, resulting in a dose in the range of 30 to 90 mSv) result in an increased risk of cancer (Brenner and Hall 2007). The evidence is reasonably convincing for adults and very convincing for children, because they are inherently more radiosensitive and because they have` more remaining years of life during which a radiation-induced cancer could develop (Brenner and Hall 2007). In addition, rapidly growing use of pediatric CT and the potential for increased radiation exposure to children undergoing these scans remain a public health concerns, a special considerations should be applied when using pediatric CT (FDA, 2017). Doses from a single pediatric CT scan can range from about 5 mSv to 60 mSv. Among children who have undergone CT scans, approximately one-third have had at least three scans. The National Cancer Institute and The Society for Pediatric Radiology developed a brochure, Radiation Risks and Pediatric Computed Tomography: A Guide for Health Care Providers, and the FDA issued a Public Health Notification, Reducing Radiation Risk from Computed Tomography for Pediatric and Small Adult Patients, that discuss the value of CT and the importance of minimizing the radiation dose, especially in children (Feigal, 2002). Concerning cardio-vascular diseases (CVDs), coronary artery disease (CAD), cerebrovascular and peripheral arterial disease included, it is to be appreciated that these are prominent causes of death. In 2016, CVDs were estimated to globally account for 31% of all deaths, 17.9 million individuals succumbing to such disease (WHO, 2019). With Vascular CT angiography now considered the gold standard for assessment of CVD, providing rapid diagnosis of patient condition, its use is expected to increase, potentially replacing digital subtraction angiography (DSA) (Liu and Platt 2014). The quantity most relevant for assessing the risk of cancer detriment from a CT procedure is the effective dose (Goldman 2007). Effective dose is evaluated in units of millisievert (abbreviated mSv; 1 mSv = 1 mGy in the case

of x rays.) Using the concept of effective dose allows comparison of the risk estimates associated with partial or whole-body radiation exposures. This quantity also incorporates the different radiation sensitivities of the various organs in the body.

Estimates of the effective dose from a diagnostic CT procedure can vary by a factor of 10 or more depending on the type of CT procedure, patient size and the CT system and its operating technique. Therefore, the patient's benefit from the accurate diagnosis is outweighing the radiation risk of radiation exposure; protection of patient from unproductive radiation exposure is recommended (Gregory, Bibbo et al. 2009).

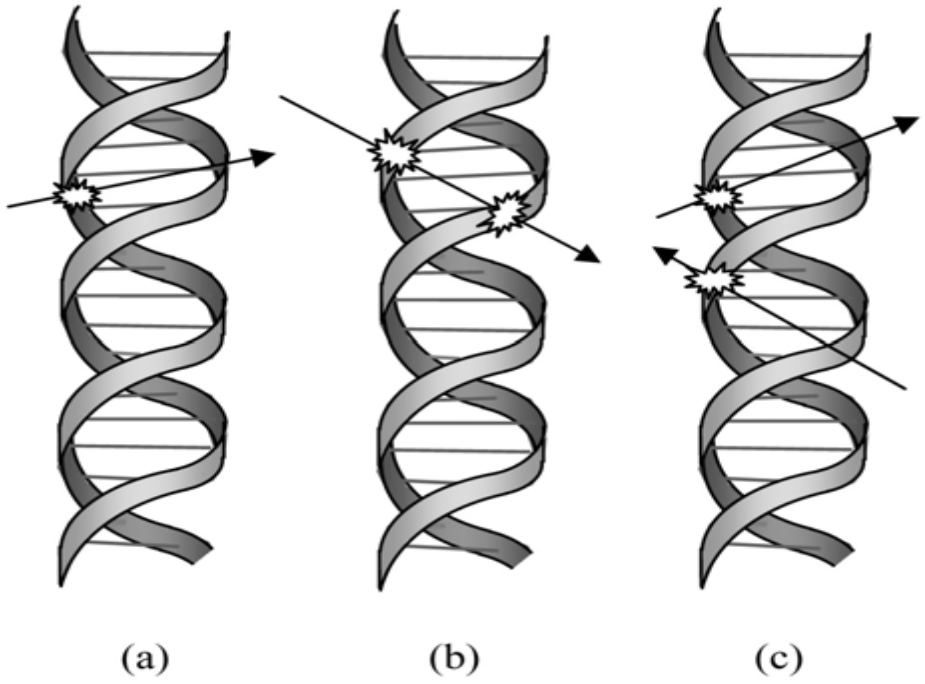

Fig (2.8): Illustration of radiation damage to DNA. (a) Single strand break. (b) Double strand break by a single event. (c) Double-strand break by two independent events .

2.1.11 CT image quality:

In any CT study, the reconstructed CT image contains quantitative information that requires precision and accuracy; precision describes the reproducibility of a measurement, and accuracy characterizes the closeness of the measurement to

the truth (AC09617961 2012). Image quality in CT as in all medical imaging devices depends mainly on four basic factors, which are image contrast, special resolution, image noise and artifact (Goldman 2007).

2.1.11.1 CT image contrast:

Image contrast in CT can be determined by subject contrast and display contrast; display contrast can be easily manipulated by using the window level and window width. The subject contrast in CT depends on the ability of tissue or subject to make differences in x-ray attenuation by absorbing or scattering of radiation, these differences in intensity of attenuated x-ray reaching the detector. The subject soft-tissue contrast in CT comes mainly from differences in physical density. Therefore, the small differences in soft-tissue density can be visualized on CT due to the nature of the image (Goldman 2007).

2.1.11.2 CT number:

The most important output from a CT scanner is the image itself, the reconstructed images represent the linear attenuation coefficient map of the scanned object, the actual intensity scale used in CT is the Hounsfield unit (HU) (Jiang 2009), named after Godfrey Hounsfield, one of the pioneers in the development of CT, these units are also referred to as CT numbers, or density values. Hounsfield arbitrarily assigned the number zero for distilled water, the number 1000 for dense bone, the number −1000 assigned for air and the values higher than 2,000 HU represented for very dense materials, such as metallic dental fillings (Romans 2018).

The CT number (HU) of any sample material can be defined by the expression:

$$HU = \ldots\ldots\ldots\ldots\ldots\ldots\ldots$$

Where $\mu_w(E)$ and $\mu_s(E)$ are the linear attenuation coefficients at the energy of the X- ray beam for water and the scanned sample respectively and K is a constant has a value of 1000 if the

CT value scale is in Hounsfield units (AC09617961 2012).

Regular quality control test for uniformity can be obtained by measuring the CT value of water using an appropriate water phantom. The accepted tolerance range for different measures over time of the mean CT value of the water phantom is usually 0 _ 4 HU and _2 HU for uniformity.

2.1.11.3 Spatial resolution:

Spatial resolution in CT, as in other modalities, is the ability to distinguish small, closely spaced objects on an image. A common test is an evaluation of limiting resolution, performed using line-pair test patterns. CT phantom line-pair patterns consist of bars of acrylic (or some denser plastic) separated by spaces containing a material that is less attenuating. The widths of the bars and spaces are equal and typically range from about 0.05 or smaller to 0.5 cm.
Resolving a line-pair test pattern requires that each bar and space be separately visible on the image. Each bar plus adjacent space is referred to as a line-pair. Rather than specifying bar width, bar pattern sizes are usually described by a spatial frequency in line-pairs per centimeter, defined as follows, where bar width is in centimeters (Goldman 2007).

$$\text{Spatial frequency} = 1 \div (2 \times \text{bar width})$$

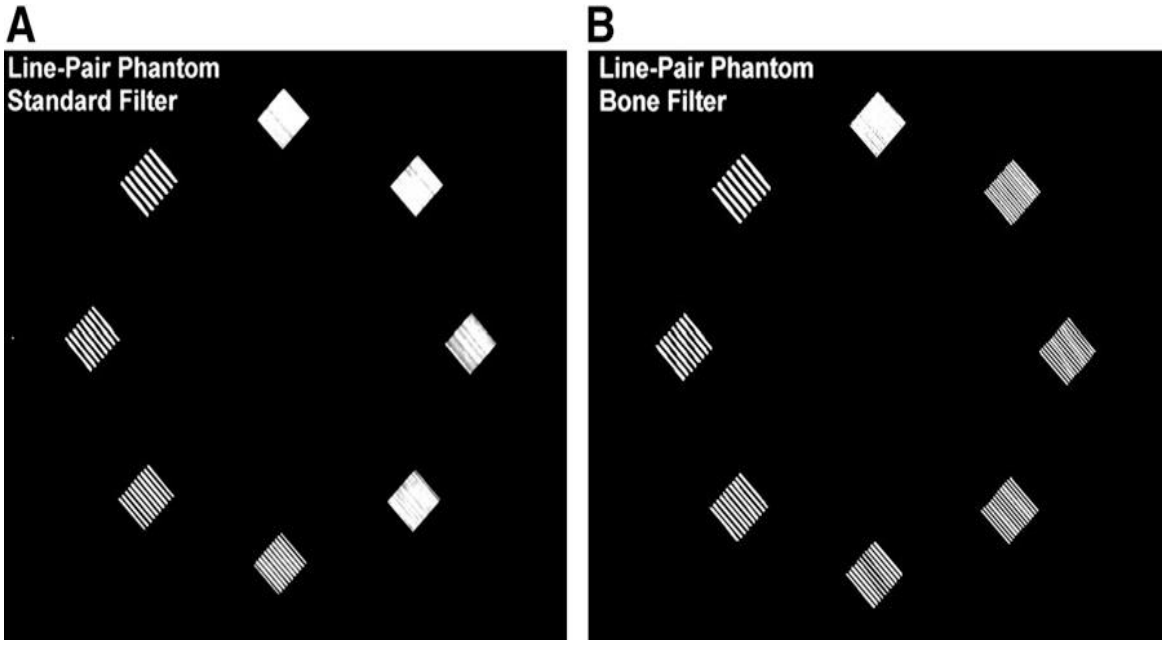

Fig (2.9): Spatial resolution of line –pair by standard filter and bone filter

Spatial resolution is the system's ability to resolve, as separate forms, small objects that are very close together. Examples of imaging challenges that depend on spatial resolution are two 1-mm-diameter iodinated contrast filled arteries that are just 1 mm apart and small bone fragments in a crushed ankle (Romans 2011).

2.1.11.4 Contrast resolution:

Contrast resolution (or low-contrast resolution) is the ability of CT scanner to differentiate a structure that varies only slightly in density from its surrounding. Such as the differentiating of a liver lesion surrounded by healthy liver tissue, in comparison to another medical imaging "CT is superior to all other clinical modalities in its contrast resolution. For comparison, in screen-film radiography, the object must have at least a 5% difference in contrast from its background to be discernible on the image. On CT images, objects with a 0.5% contrast variation can be distinguished" (Romans 2011).

2.1.11.5 Image noise:

Image noise is the undesirable fluctuation of pixel values in an image of a homogeneous material. If an image is created of an object that is known to be uniform in density, such as a water phantom, then all measured points within that image should in theory be the same, but in practice they are not (Romans 2011). When a uniform material is imaged on CT scanner, the examinations of CT values for individual pixels in a localized area shows that the CT numbers are not all the same, but fluctuate around a mean value (AC09617961 2012), the standard deviation (SD) measurement is an indication of the amount of variance among pixel values in a designated region of interest (ROI), The SD measurement of an ROI of a known uniform phantom will indicate the degree of noise in an image, the smaller the SD, the less the noise and the better the contrast resolution capability (Romans 2011). This random variation is known as image noise and is due primarily to the statistical nature of X- ray production and interaction with matter. It is also known as quantum noise (AC09617961 2012).

2.1.11.6 Signal to noise ratio:

The signal to noise ratio is the measure of delectability of the object in noisy image, the signal to noise ratio in the region of interest can be measured by the ratio of mean gray value of the region of interest to the noise in that region.

2.1.11.7 Contrast to noise ration:

CT scanning utilizes a large photon flux in acquisition in order to achieve low noise images. However, this results in higher patient doses. These images allow the identification of low contrast structures, reflecting very small differences in photon attenuation in the tissue due to composition or density differences. While the image noise in a uniform material is usually a good indicator of the ability to

visualize small contrasts in diagnostic images, a more versatile measure is that of CNR. To measure CNR, the contrast of two objects is determined by the difference of the mean CT numbers within selected ROIs and is divided by the average noise for these two ROIs:

$$CNR = \ldots\ldots\ldots\ldots\ldots$$

This parameter is useful when optimizing a CT examination protocol for a particular contrast situation e.g. tissue density contrast, iodine contrast and air tissue contrast.

2.1.12 Detectors efficiency:

X-ray detector element is typically an ionization chamber using high pressure xenon or a scintillation detector. Early scanners used scintillation detectors such as sodium iodide (NaI) or cadmium tungstate (CdWO4); later high pressure xenon generally replaced these early materials and in later years scintillator doped ceramics have been used, such as gadolinium oxysulphide (Gd2O2S) or yttrium gadolinium oxide (YGdO). Important specifications for such detector elements, and factors in their development, include a high dynamic range, high quantum absorption efficiency and a fast temporal response with low afterglow. For a single slice axial scanner, the detector unit will have over 700 elements arranged along an arc to intersect the exit beam of the topographic plane. This is known as 3rd generation scan geometry which is the basic design of modern CT scanners. In multi-detector CT scanners, the detector typically has additional adjoining arcs, or rows, of detector elements. Such multi-row detectors may have up to 64 rows, allowing total acquisition width 2 of 32– 40 mm (measured at the isocentre). This type of acquisition can produce slice thicknesses varying from 0.5 mm to 10 mm. With such a detector, the acquisition time is reduced and the occurrence of motion artifacts' is considerably reduced (AC09617961 2012).

2.1.13 CT dose optimization:

Justification and optimization of medical radiological examinations are the tow key elements for radiation dose reduction, justification is tended to ensure that patients benefit from the procedure exceed any potential of risk from exposure to ionizing radiation, optimization is a process of obtaining desired image quality of answering the diagnostic task with a minimum amount of radiation dose (Protection 1996). Patient's benefit from the accurate diagnosis outweighs the radiation risk of radiation exposure, protecting the patient from unproductive radiation exposure is recommended (Gregory et al. 2009). Unproductive radiation exposure may be delivered when the image acquisition parameters are not adequately attuned to patient size (Elnour, Yousef, et al. 2015). Therefore, when a CT scan is justified by medical need, the associated risk is small relative to the diagnostic information obtained (Brenner and Hall 2007). Therefore, about 20 million of adults CT examinations and more than 1 million of children CT examinations per year in the United States are being irradiated unnecessarily (Brenner and Hall 2007). In addition, organs and tissues lying outside the field of interest may also be susceptible to secondary radiation such as breast tissue, the sensitivity of which has been emphasized in the latest International Commission on Radiological Protection recommendations. To monitor clinical practice, DRLs firstly introduced in 1996 by International Commission on Radiological Protection (ICRP) Publication 73 and then the concept was subsequently developed further and further clarified as a dramatically development of the concept, a practical guidelines was introduced in 2001(Vañó, Miller et al. 2017). "Diagnostic reference levels (DRLs) are benchmarks for radiation protection and optimization of patient imaging, and it can be defined as an investigational level that applies to an easily measured quantity using a standard phantom or representative patient"(Kanal, Butler et al. 2017). The use of DRLs is endorsed by professional, advisory, and

regulatory organizations, including the ICRP, American College of Radiology (ACR), AAPM, United Kingdom Health Protection Agency, International Atomic Energy Agency, and European Commission.

DRLs are typically set at the 75th percentile of the dose distribution from a survey conducted across a broad user base (ie, large, small, public, private, hospital, and outpatient facilities) using a specified dose measurement protocol (Kanal, Butler et al. 2017). DRLs are suitable tools for indicating the practical level in the country as well as in the region (Vassileva and Rehani 2015). By comparing them the elevated radiation dose can be identified, then the suitable modification for dose optimization can be applied. Therefore, the establishments of national or regional DRL is helpful for addressing the variations of different protocols between different facilities (Vassileva and Rehani 2015).

2.1.14 Contrast agent in CT:

The tissues on a CT image must have different densities (attenuation) to be differentiated. These varying densities will result in distinct attenuation coefficients, which produce an image that displays the different tissues (Romans 2011). In some parts of the body, such as the chest, subject contrast is inherently high. The pulmonary vessels and ribs have significantly different densities from the adjacent aerated lung, allowing easy image identification. Unfortunately, not all body areas possess this level of inherent tissue contrast. Often, many tissues have quite similar attenuation coefficients. In addition, tumors and other disease processes may have attenuation coefficients that are very similar to their surrounding tissues (Romans 2011). For this reason, contrast agents have been developed that are highly visible in an x-ray or CT scan and are safe to use in patients. Contrast agents contain better substances at stopping x-rays and, thus, are more visible on an x-ray image. (Turning Discovery intoHealth. 2019). An oral or intravenous contrast agent administration is often used to create a temporary, artificial density difference between objects. The goal is to give

different tissues, which would ordinarily have similar attenuations, different attenuation coefficients, making them more readily visible on the image. Methods of contrast administration vary widely, but in CT, enhancement falls into the two main categories of intravascular and gastrointestinal. Less commonly, contrast agents can be administered intrathecally (into the subarachnoid space surrounding the spinal cord) or intra articularly (directly into a joint space). In all categories, contrast agents fill a structure with a material with a different density than that of the structure. In the case of most agents that contain barium and iodine, the material is of a higher density than the structure. These are typically referred to as positive agents. Low-density contrast agents, or negative agents, such as air or carbon dioxide, can also be used. Specific gastrointestinal agents possess a density similar to water and are sometimes referred to as “neutral” contrast agents (Romans 2011). The Contrast agents play an essential role in CT imaging. Without contrast media, many structures and disease processes would be indistinguishable. Although there are many diagnostic benefits associated with the administration of contrast media, they also have the potential to cause patients harm (Romans 2011).

2.2 Previous Studies:

Different clinical applications require different X-ray spectra and hence different kV settings for optimum image quality and/or best possible signal to noise ratio at lowest radiation dose. the benefit of low kV settings can be achieved in Contrast enhanced CT scan using iodinated contrast agent, in particular CT angiographic examinations, because of the increased iodine contrast at lower kV, the contrast to noise ratio (CNR) in contrast enhanced images increases at low kV if the radiation dose is kept constant (McCollough, Primak et al. 2009). Qurashi reported 40% dose reduction in the use of 100 KV instate of 120 KV, the associated noise increase was improved by SAFIRE (5) in 60% noise reduction compared to FBP When combined with iterative

reconstruction, the low kV is feasible for obese patients to optimize radiation dose without compromising objective image quality ((Qurashi, Rainford et al. 2019). In the same way, McCollough was listed several factors for appropriate application of lower kV techniques (McCollough, Primak et al. 2009). These factors are: firstly, increased mAs have to be used to avoid excessive noise level, because of the less efficient x-ray production of the tube at low kV values. Secondly, a weight or size-based kV/mAs technique chart should be used for achieve appropriate at lower kV scanning for certain patient size. Thirdly, motion artifacts and decreased scan time for pediatric patients can be avoided by applying high helical pitch and fast rotation time. Which is often limits the maximum mAs due to the limitation of the tube current. To adders this limitation it is necessary raise up the KV to avoid compromising the image quality. Lastly, lower kV increases the contrast of iodine; it may not increase the contrast of tissues, lesions, and other pathologic structures without iodine uptake. The use of lower kV has to be carefully evaluated by radiologists and physicists for every particular type of pediatric examination. Therefore, Because of limitations of the X-ray tube current low kV protocols have so far been limited to small patients and children. Also different studies have been reported remarkable reduction in radiation dose by applying iterative reconstruction technique. In a larger study on 55 pediatric cardiac patients, SAFIRE was found to significantly reduce image noise by 35% and improve qualitative assessment of image noise and noise texture (Raupach 2012). In recent study, Cianci reported 63% of dose reduction in ultra-low dose (ULD)-CT colonography (CTC) obtained with the combined use of automatic tube current (mAs) modulation with a quality reference mAs of 25 and (SAFIRE), compared to low-dose (LD) CTC acquired with a quality reference mAs of 55 reconstructed with filtered back projection (FBP), the image noise remain comparable (Cianci, Delli Pizzi et al. 2019). AIDR 3D can be routinely applied to all clinical

acquisition modes and is able to remove up to 50% of image noise, while maintaining image quality, and resulting in dose reduction of up to 75% (Geleijns and Irwan 2012). Tang, et al has been found mean dose reduction of 57.8% for AIDR 3D algorithm integrated with automatic tube current modulation as compared with filtered back projection (FBP), a consistent noise level without sacrificing coronary artery calcium score CACS was reported (Tang, Liu et al. 2018). Nakamoto et al were studied the diagnostic ability of low tube voltage and reduced contrast material dose hepatic dynamic computed tomography (CT), in use of AIDR 3D, they found a reduction in radiation dose and in the amount of contrast material without degradation of diagnostic performance as compared with filtered back projection FBP (Nakamoto, Yamamoto et al. 2018). Mello-Amoedo, et al 2018, have been obtained significant radiation dose reduction in patients who underwent abdomen-pelvic CT examinations with portal venous phase, by applying AIDR 3D a mean dose reduction of 62.5% , 58% and 63% in CTDIvol , ED, and SSDE was found respectively as compared with filtered back projection FBP without compromising diagnostic image quality (Mello-Amoedo, Martins et al. 2018). Zhang (Zhang, Chen et al. 2019), reported a remarkable improved image quality for AIDR3D in low-radiographic dose head and neck CTA over FBP, the low-dose CTA images proved all requirements of clinical diagnostic tasks. Overview of diagnostic reference level values for different countries from literature survey were also reported, variations in DRLs of abdomen- pelvic multi-phase CT examination was observed. For example, the lowest DRLs (75%) values in terms of CTDIvol and DLP were observed in U.S which are 19 mGy and 995 mGy.cm respectively (Kanal, Butler et al. 2017). in United Arab Emirates 20.4 mGy and 1023.1 mGy.cm respectively (Abuzaid, Elshami et al. 2020) and the highest values was observed in Japan it was elevated from 15 mGy and 1800 mGy.cm in 2015 (Yonekura, 2015) to 17 mGy and 2100 mGy.cm in 2020

(Kanda, Akahane et al. 2020). European Union E.U DRLs was 15 mGy and 1800 mGy.cm for CTDIvol and DLP respectively (E.U 2014), in Ireland was 12.6 mGy and 1115 mGy.cm (Foley, McEntee et al. 2012). and in Korea (Kim, Lee et al. 2019) reported the values ranging between 7.5 mGy and 10.58 mGy and 939.07 mGy.cm and 1511.41 mGy.cm for 1stQ and 3rd Q values of CTDIvol and DLP respectively. In Egypt (Salama, Vassileva et al. 2017) reported DRLs values of 33 mGy and 1320 mGy.cm for CTDIvol and DLP respectively. Recently, in Switzerland, (Aberle, Ryckx et al. 2020) was reported DRLs values for first quartile and third quartile of CTDIvol and DLP by 7 mGy and 830 mGy.cm and 11 mGy and 1170 mGy.cm. The diagnostic reference level reported by ICRP 87 for adult in CT for routine abdomen is 35 mGy for CTDIvol and 780 mGy.cm for DLP (ICRP 87). European guideline on quality criteria for computed tomography reported reference dose value for routine abdomen by 35 mGy and 780 mGy.cm for CTDIvol and DLP respectively (EUR16262). The American association of physicist in medicine also reported 50 mGy of CTDIvol for adult torso (AAPM, 2011). In American College of Radiology (ACR) the reference level of CTDIvol for adult abdomen is 25 mGy (ACR 2008). These examples of DRLs for contrast enhanced multi-phase abdominal CT studies reported by previous studies from different countries in the region and worldwide were considered a base line for establishment of national DRLs for contrast enhanced multi-phase abdomen-pelvic CT examination in Sudan.

Also, different studies reported radiation dose parameters in term of CTDIvol and DLP mGy.cm for pediatric patient underwent abdominal CT studies; (Kritsaneepaiboon et al. 2012) reported 16.8 mGy and 764 mGy.cm for CTDIvol and DLP for multi-phase pediatric abdomen CT examination in Thailand. In Switzerland (Verdun et al. 2008) reported values of CTDIvol and DLP for pediatric as 16 mGy and 500 mGy.cm respectively. (Granata et al.

2014) reported 14 mGy of CTDIvol and 602 mGy.cm of DLP for Italian pediatric patient. In Germany (Galanski et al. 2007) reported 10.1mGy and 402 mGy.cm for CTDIvol and DLP respectively, comparable value of CTDIvol and DLP also reported by Watson (Watson & Coakley. 2010) in Australia as 10 mGy and 318 mGy.cm respectively. (Kim et al. 2017) reported 8.3 mGy and 491mGy.cm for Korean abdomen pediatric CT study. In recent study, CTDIvol of 3.8 mGy and DLP of 180mGy.cm were reported in France by Celier (Celier et al. 2020). All these evidence can be used in the determination of our situation in the clinical practice of multi-phase abdomen CT examination.

Table (2.1): show 1st quartile and 3rd quartile values of CTDIvol (mGy) and DLP (mGy.cm) of adult patients of previous studies

DRLs for different countries	1st Quartile (25%)		3rd Quartile (75%)	
	CTDIvol mGy	DLP (mGy.cm)	CTDIvol mGy	DLP (mGy.cm)
Ireland 2012 (Foley, McEntee et al. 2012)	N.A*	N.A*	12.6	1115
Korea 2019 (Kim, Lee	7.05	939.07	10.58	1511.41

et al. 2019)				
EU 2014	N.A*	N.A*	15	1800
Japan 2015 (Yonekura, Yoshiharu. 2015)	N.A*	N.A*	15	1800
Japan 2020 (Kanda, Akahane et al. 2020)	N.A*	N.A*	17	2100
U.S 2017 (Kanal, Butler et al. 2017)	N.A*	N.A*	19	995
United Arab Emirates 2020 (Abuzaid, Elshami et al. 2020)	13.3	533.6	20	1025
Egypt 2017 (Salama, Vassileva et al. 2017)	N.A*	N.A*	33	1320
Switzerland 2020 (Aberle, Ryckx et al. 2020)	7	830	11	1170

N.A* = Not Available

Table 2.2 shows mean values of CTDIvol (mGy) and DLP(mGy.cm) for pediatric patient of previous studies.

Auther, Year	**Country**	**CTDIvol (mGy)**	**DLP (mGy.cm)**
Celier et al. (2020)	France	3.8	180
Kim et al. (2017)	Korea	8.3	491
Granata et al. (2014)	Italy	14	602
Kritsaneepaiboon et al. (2012)	Thailand	16.8	764

Watson & Coakley. (2010)	Australia	10	318
Verdun et al. (2008)	Switzerland	16	500
Galanski et al. (2007)	Germany	10.1	402

CHAPTER THREE

MATERIALS and METHODS

CHAPTER THREE

MATERIALS and METHODS

3.1 Materials :

3.1.1 Computed tomography (CT) scanners:

Nine different modalities of CT scanners having detectors row ranging from 16 to 160 slices configured in nine different hospitals were used in this study (table 3.1). All quality controls for the CT machines were carried out by experts from Sudan Atomic Energy Commission (SAEC) before any data collection.

Table 3.1: Show CT modalities in different diagnostic centers

Hospital	manufacture	model	Year of installation	Detector type
A	Siemens GE	Bright speed	2010	16 slice
B	Siemens GE	Optima CT 520	2017	16 slice
C	Toshiba	Aquiline prime TSX-303A	2016	160 slice
D	Neusoft	NeuVize	2011	16 slice
E	Neusoft	NeuVize	2016	128 slice
F	Toshiba	Toshiba Aquiline	2010	64 slice
G	Siemens	sensation	2007	16 slice
H	Toshiba	Aquiline CGGT-032A	2016	160 slice
I	Toshiba	Toshiba Aquiline	2012	64 slice

3.1.2 Data collection survey form:

Two different data collection survey form were prepared for collecting data of this study. First one for collecting data of scanners specifications (manufactures, model, detector type and year of installation) and the second form for collecting patient demographic data and patient exposure related parameters (Appendix 1 & Appendix 2).

3.1.3 Data analysis software:

Microsoft office excel 2007 soft ware program and OriginLab software (Originpro 8, 2007) were used for the analysis and graphing of collected data.

3.2 Methods:

3.2.1 Patient data:

A total of 642 (adults and pediatric) patient's demographic data of patients undergoing abdominal contrast enhanced CT examinations were collected from nine diagnostic centers in Khartoum state Sudan (table 3.2).

Data of the technical parameters used in the CT procedure for estimation purposes were taken from 1st March 2017 to 30th April 2018. Moreover, data for optimization purposes were taken from 1st June 2018 to 12th May 2019.

In the first stage of the study, data of 514 adult patient underwent abdomen contrast enhanced CT examination performed by using departments' protocol (standard technique) were collected from nine hospitals for situation analysis of the current practice without any modifications of imaging parameters for dose optimization purpose.

In the second stage of the research, we use tow different vendor technique introduced by Toshiba to optimizing radiation dose. These techniques are a modification of full sure exposure low dose technique protocol and a modification of combination of sure exposure 3D low dose technique with standard and/or high-quality technique protocol.

43 studies were performed by using a Combination protocol (low dose with standard and/or high quality technique) and 56 studies were performed by using 3D sure exposure low dose technique.

Pediatric patients also have been considered in this study, a total of 58 pediatric patients without any modification for dose optimization were collected from six different hospitals conducting pediatric CT examination.

Data were collected to study the effect of patient-related parameters (e.g. age, sex, diagnostic of examination, and use of contrast media). and exposure-related parameters (gantry tilt, kilo voltage (kV), tube current (mA), exposure time, slice thickness, table increment, number of slices, and start and end positions of scans) on patient dose.

The collection of data was done by using patient dose survey form prepared for data collection of patient exposure-related parameters (Appendix 2).

3.2.2 Imaging protocols:

The exposure parameters remain constant, KVp ranged from 100 to 120 KVp, reference mAs automatic exposure control (AEC), 0.5 second rotation time, 5 mm slice thickness and 65 helical pitch were used in all phases of examination.
Noise of desired image quality for optimization purpose in hospital (C) was suppressed from 7.5 for standard protocol to 9 for high quality protocol and 12.5 for sure exposure low dose protocol.

Table 3.2: show the study population in different hospitals.

Diagnostic center/Hospital	No. of patients (adult)	No. of patients (pediatric)	total
A	55	14	69
B	62	10	72
C	102	10	112
C*	43	-	43
C**	56	-	56
D	58	-	58
E	56	8	64
F	32	10	42
G	49	6	55
H	49	-	49
I	22	-	22
Total	584	58	642

C= standard technique, C*= combination technique, C**= low dose technique and

3.2.3 Methods of evaluation of CT radiation dose:

CTDIvol (mGy) and DLP (mGy.cm) for every single phase and total DLP (mGy.cm) for all phases for complete examination were measured by the scanner software displayed on monitor as the summary of dose.

The averages of total DLP (mGy.cm) for complete examination were calculated as an average DLP (mGy.cm) for complete contrast enhanced multiphase abdominal CT examination.

3.2.4 Calculation of DRLs:

1st quartile, 3rd quartile and inter quartile range of CTDIvol and DLP were calculated as the diagnostic reference level for contrast enhanced abdominal CT in Sudanese hospitals.

3.2.5 Effective dose estimation:

DLP to E "k" Conversion Coefficients introduced in 2004 by EC (European Commission) and 2005 by NRPB (National Radiological Protection Board) was used to estimate the effective dose which is found as 0.015 for abdomen.
For pediatric patients, effective dose per dose length product (E/DLP) values for abdomen and pelvis obtained by Shrimpton were used as DLP to E conversion factor for specific age group, as well as, 0.049 for 0 year old, 0.030 for 1 year old, 0.020 for 5 years old and 0.015 for 15 years old (Shrimpton, P. 2004). The average effective dose in (mSv) for complete contrast-enhanced abdominal multiphase CT examination was estimated by the product of total DLP with the "k" conversion coefficients.

$$E = k \times DLP$$

3.2.6 Cancer risk estimation:

The resultant cancer risk (RCR) per procedure was estimated by multiplying effective dose with the risk coefficient factor (RCF) introduced by ICRP 103 which is $5.5*10^{-2}$ Sv as follows:

$$RCR = RCF * Eeff$$

3.2.7 Image quality analysis:

The most important parameters have direct effect on the image quality are the radiation dose and the level of the noise, to perform quantitative image analysis in term of signal-to-noise ratio (SNR), the mean value of the density within the ROI (HU) and its standard deviation (SD) were measured by using three different identical circular regions of interest (ROIs of ≥ 100 mm^2) set in the organs of interest of normal (lung, liver and bone) for 10 samples in three different protocol, then SNR was calculated by dividing the Hounsfield value by the noise value (HU/SD).

The percentage different formula was used to evaluate the change in radiation dose reduction.

$$PD = [| V1\text{-}V2 | \div \quad] \times 100$$

For qualitative image quality analysis, more than 10 radiologists (3 to 10 years of experience) participated in diagnostic of out sorted images.

CHAPTER FOUR

RESULTS

CHAPTER FOUR

RESULTS

4 Results:

The results of this study collected from 642 patients (adult & pediatric) underwent multi-phase contrast enhanced abdominal CT examinations conducted in nine hospitals by using different vendors of CT machine (Table 3.1), the results were classified in different tables according to the study protocol (standard protocol, combination of low dose with standard dose and/or high quality dose protocol and low dose protocol).

4.1 Study population and patient's demographic data:

Table (4.1) presents the results of adult patients' demographic data of standard protocol (current practice) in nine hospitals.

DC / hospital code	Gender (adult)			Age (year)		
	Male	Female	Total	Mean	Standard deviation	Range (min – max)
A	22 (40%)	33 (60%)	55	47	21	18 – 85
B	25 (40%)	37 (60%)	62	49	17	18 – 87
C	54 (53%)	48 (47%)	102	55	17	20 – 90
D	16 (27.6%)	42 (72.4%)	58	52	16	18 – 81
E	24 (42.9%)	32 (57.1%)	56	51	16	22 – 80
F	16 (50%)	16 (50%)	32	55	19	19 – 93
G	25 (51%)	24 (49%)	49	46	18	45 – 84

DC / hospital code	Gender (adult)			Age (year)		
	Male	Female	Total	Mean	Standard deviation	Range (min – max)
H	26 (53%)	23 (47%)	49	46	18	18 – 89
I	10 (45.5%)	12 (54.5%)	22	53	19	28 – 85
Total	218 (45%)	267 (55%)	485	50	18	18 – 93

Table (4.2) presents the results of pediatric patients' demographic data of standard protocol (current practice) in six hospitals.

DC/ hospital code	Gender (pediatric)			Age (year)		
	Male	Female	Total	Mean	Standard deviation	Range (min – max)
A	14 (100%)	NA*	14	8	3	6 – 12
B	10 (100%)	NA	10	6	3	4 – 10
C	4 (40%)	6 (60%)	10	12	4	5 – 15
E	8 (100%)	NA*	8	6	5	1 – 12
F	6 (60%)	4 (40%)	10	5	2	2 – 7
G	2 (33%)	4 (67%)	6	15	1	15 – 15
Total	44 (76%)	14 (24%)	58	9	3	1 – 15

- NA* = Not available

Table (4.3) present results of adult patients' demographic data conducted in hospital C by using two different study protocol for radiation dose optimization purpose.

DC / hospital code	gender			Age (year)		
	Male	Female	Total	Mean	Standard deviation	Range (min – max)
C*	10 (23%)	33 (77%)	43	54.47	15.51	27 – 95
C**	19 (34%)	37 (66%)	56	53.09	17.05	19 – 80
Total	29 (29.3%)	70 (70.7%)	99	53.78	16.28	19 – 95

C*= combination of low dose technique with standard and/or high quality dose technique

C**= low dose technique

4.2 Radiation dose parameters:

CT radiation dose parameters were studied in terms of CTDIvol (mGy) and DLP (mGy.cm).

Table 4.4 present the results of CTDIvol of standard dose protocol (current practice) for adult patients' in nine hospitals.

DC code	CTDIvol mGy (Mean ± SD)	Range (Min – Max)	1st Quartile (Q1)	3rd Quartile (Q3)	Interquartile Range (Q3 - Q1)
A	8.51 ± 3.62	(3.64 – 22.51)	6.39	10.84	4.45
B	9.2 ± 2.09	(4.63 – 12.55)	7.88	10.79	2.92
C	7.22 ± 2.29	(5.04 – 17.62)	5.7	7.93	2.23
D	19.89 ± 0.01	(19.88– 19.89)	19.89	19.89	0.00
E	9.03 ± 3.51	(3.64 – 21.23)	5.95	11.2	5.25
F	23.99 ± 4.2	(12.9 – 28.18)	22.69	28.18	5.48
G	7.04 ± 2.36	(3.23 – 14.78)	5.58	7.8	2.22
H	6.21 ± 4.41	(3.3 – 27.8)	4.43	5.84	1.42
I	24.8 ± 2.29	(19.5 – 28.5)	23.28	25.65	2.38
Total	12.88 ± 2.75	(3.3 – 28.18)	11.31	14.24	2.93

Table 4.5 present the results of DLP mGy.cm for complete procedure of standard dose protocol (current practice) for adult patients' in nine hospitals.

DC code	DLP mGy.cm (Mean ± SD)	Range (Min – Max)	1st Quartile (Q1)	3rd Quartile (Q3)	Interquartile Range (Q3 - Q1)
A	1703.76 ± 830.78	(689.68 – 4595.6)	1179.46	2231.55	1052.09
B	1417.81 ± 379.65	(636.03–2228.47)	1177.53	1661.85	484.32
C	1324.41 ± 605.4	(302.7 – 4504.8)	959.2	1512.1	552.9
D	4051.4 ± 991.04	(2329.34–8774.8)	3582.55	4179.04	596.49
E	1999.07 ± 796.07	(941.5 – 4204.9)	1281.2	2565.35	1284.15
F	4926.42± 1181.28	(2219.9 – 7873.5)	4014.15	5656	1641.85
G	1526.63 ± 635.02	(646 – 3432)	1134	1924	970
H	1365.78± 1387.72	(257 – 9263.5)	846.5	1379.3	532.8
I	4683.32 ± 1055.2	(1837.7 – 6656.4)	4593	5196.4	603.4
Total	2555.4 ± 873.57	(257 – 9263.5)	2085.29	2922.84	857.56

Table 4.6 present the results of DLP mGy.cm of single phase of standard dose protocol (current practice) for adult patients' in nine hospitals.

DC code	DLP mGy.cm (Mean ± SD)	Range (Min – Max)	1st Quartile (Q1)	3rd Quartile (Q3)	Interquartile Range (Q3 - Q1)
A	399.98 ± 186.75	(172.42–1148.9)	275.22	517.3	242.08
B	414.14 ± 101.23	(200.89 –580.25)	352.71	479.63	126.92
C	287.67 ± 124.14	(65.3 – 750.8)	209.04	338.48	129.08
D	992.15 ± 229.18	(776.45 –2193.7)	895.64	1014.85	119.22
E	491.09 ± 196.92	(227.68–1051.23)	316.95	645.3	328.35
F	1218.4 ± 213.69	(739.97 –1621.65)	1081.88	1347.68	265.8
G	357.83 ± 145.22	(129.2 – 917)	271	387	116
H	316.12 ± 230.63	(128.5 – 1323.36)	217.63	292	74.37
I	1157.51±225.52	(459.43 –1468.78)	1106.73	1299.1	192.38
Total	626.1± 183.7	(65.3 – 2193.7)	525.2	702.37	177.13

Table 4.7 present the results of effective dose and cancer risks for complete procedure of standard dose protocol (current practice) for adult patients' in nine hospitals.

DC code	DLP (mGy.cm) complete examination	Effective dose (mSv)	Cancer risk per procedure * 10-5 Sv
A	1703.76	25.56	141
B	1417.81	21.27	117
C	1324.41	19.87	109
D	4051.4	60.77	334
E	1999.07	29.99	165
F	4926.42	73.9	406
G	1526.63	22.9	126
H	1365.78	20.49	113
I	4683.32	70.25	386
Total	2555.4	38.33	211

Table 4.8 present the results of CTDIvol mGy and DLP mGy.cm for complete procedure of combination of low dose with standard or high quality dose and sure exposure low dose protocol for adult patients' in hospital C.

Modification technique	Exposure parameter	(Mean ± SD) (minimum – maximum)	1st Quartile (Q1)	3rd Quartile (Q3)	Interquartile Range (Q3 - Q1)
Combination (low dose + standard and/or high quality)	CTDIvol mGy	7.01 ± 3.05 (4 – 15.23)	5	8.35	3.35
	DLP mGy.cm	1331.48 ± 594.64 (708.5 – 3279)	893.3	1666.2	772.9
3D sure exposure low dose	CTDIvol mGy	5.2 ± 1.55 (2.6 – 9.78)	4.15	6.58	2.43
	DLP mGy.cm	811.8 ± 156.76 (482.7 – 1155.8)	679.35	939.55	260.2

Table 4.9 present the results of mean effective dose and cancer risks for complete procedure of standard dose protocol (current practice) for adult patients' in nine hospitals.

DC code	DLP (mGy.cm) complete examination	Effective dose (mSv)	Cancer risk per procedure * 10-5 Sv
C*	1331.48	19.97	110
C**	811.8	12.18	67

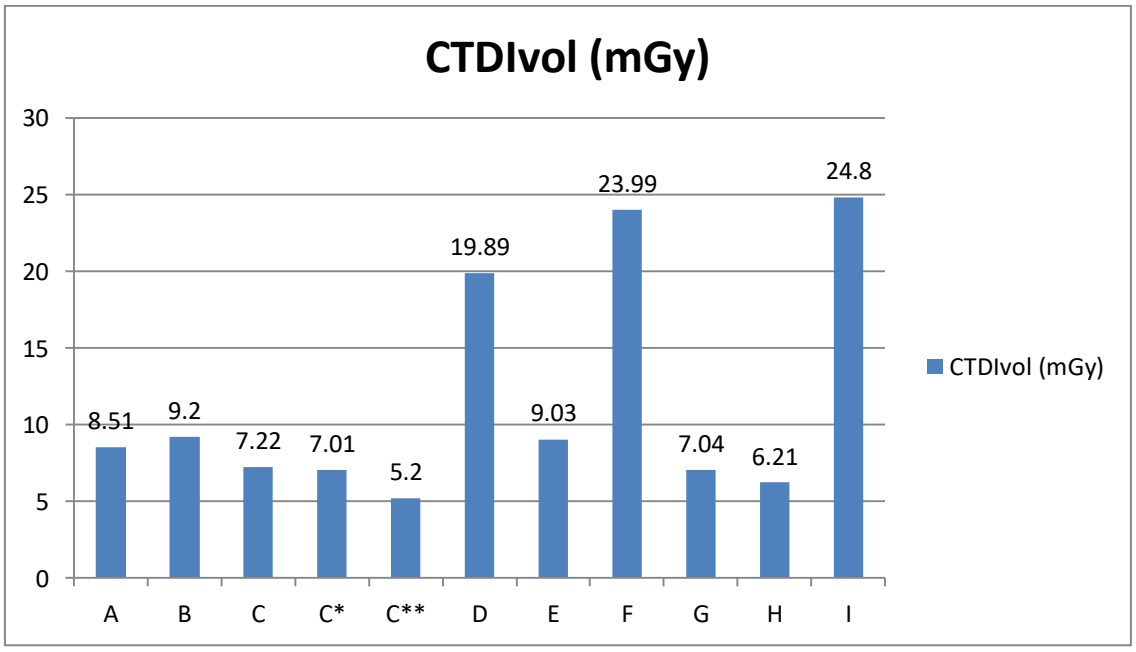

Fig (4.1): show the mean CTDIvol (mGy) for adult patient in nine hospitals/diagnostic centers. (C*= combination of low dose with high quality or standard dose, C**= pure low dose and the rest standard dose protocol)

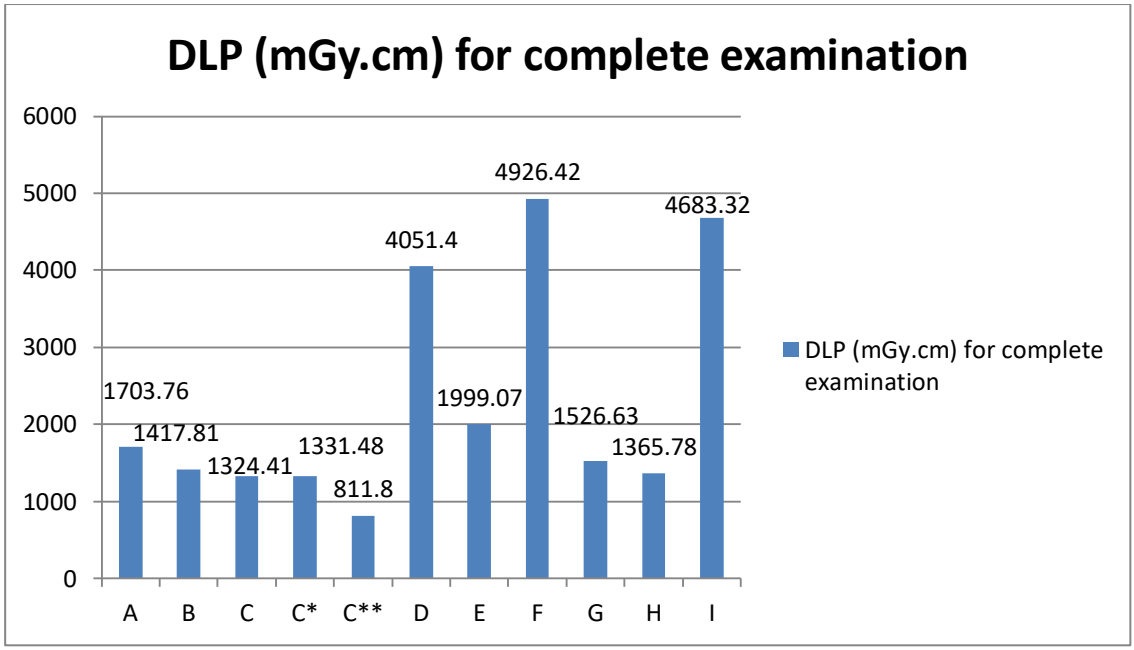

Fig (4.2): show the mean DLP (mGy.cm) for adult patient in nine hospitals/diagnostic centers. (C*= combination of low dose with high quality or standard dose, C**= pure low dose and the rest standard dose protocol).

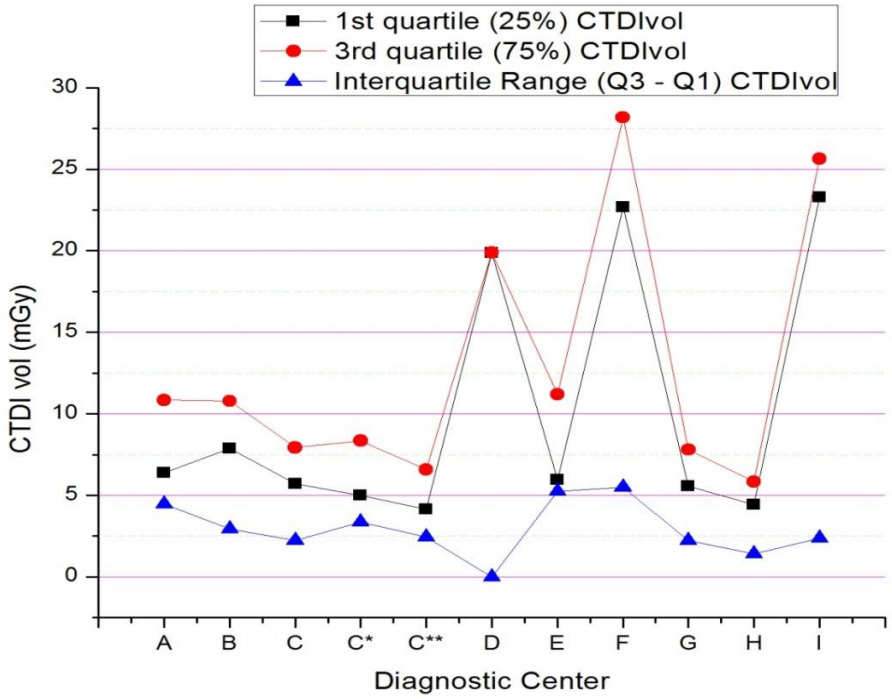

Fig (4.3): show the 1st quartile, 3rd quartile and interquartiles range for CTDIvol (mGy) for adult patient in nine hospitals/diagnostic centers.

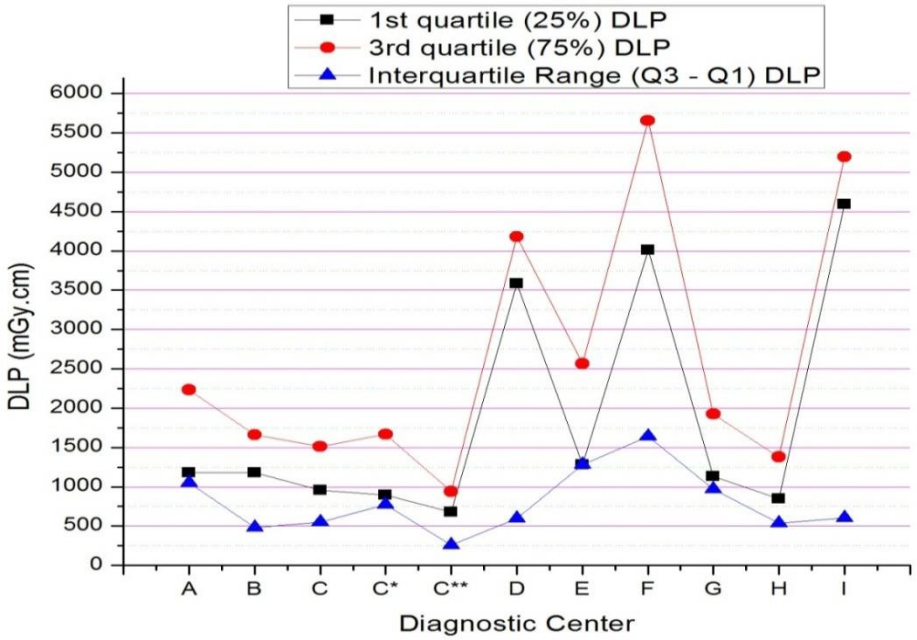

Fig (4.4): show the 1st quartile, 3rd quartile and interquartiles range for DLP (mGy.cm) for adult patient in nine hospitals/diagnostic centers.

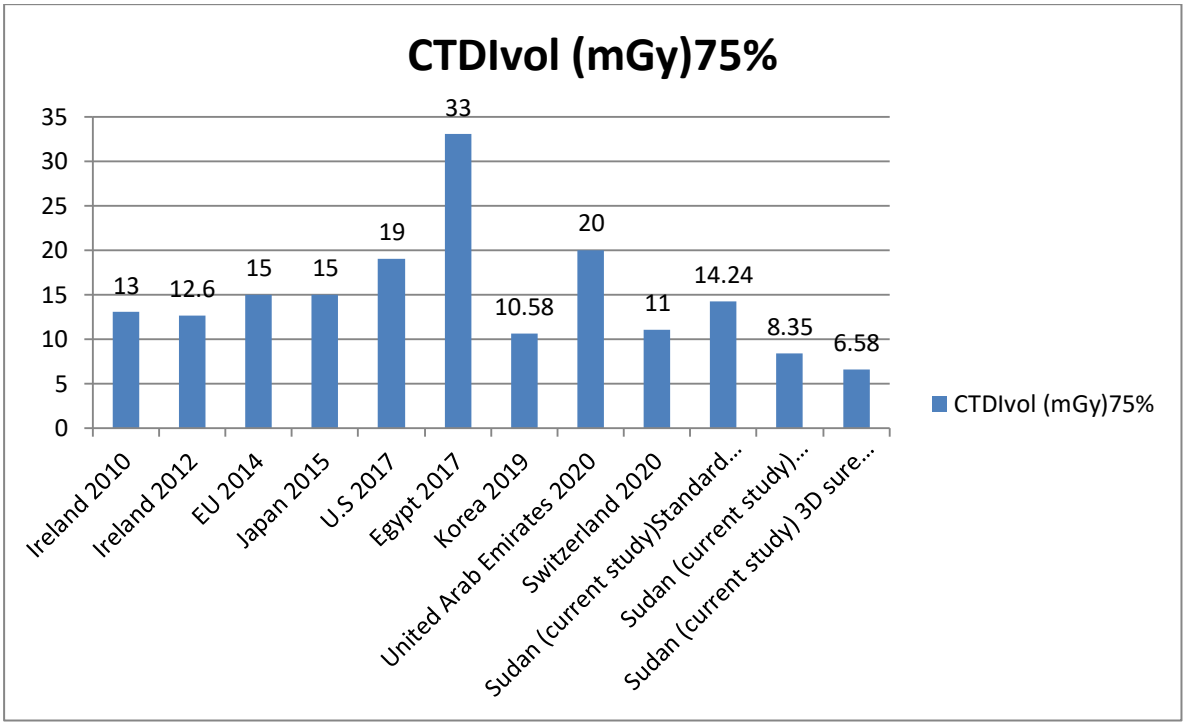

Fig (4.5): show 75% of $CTDI_{vol}$(mGy) for abdomen multi-phase study in different country and percent study.

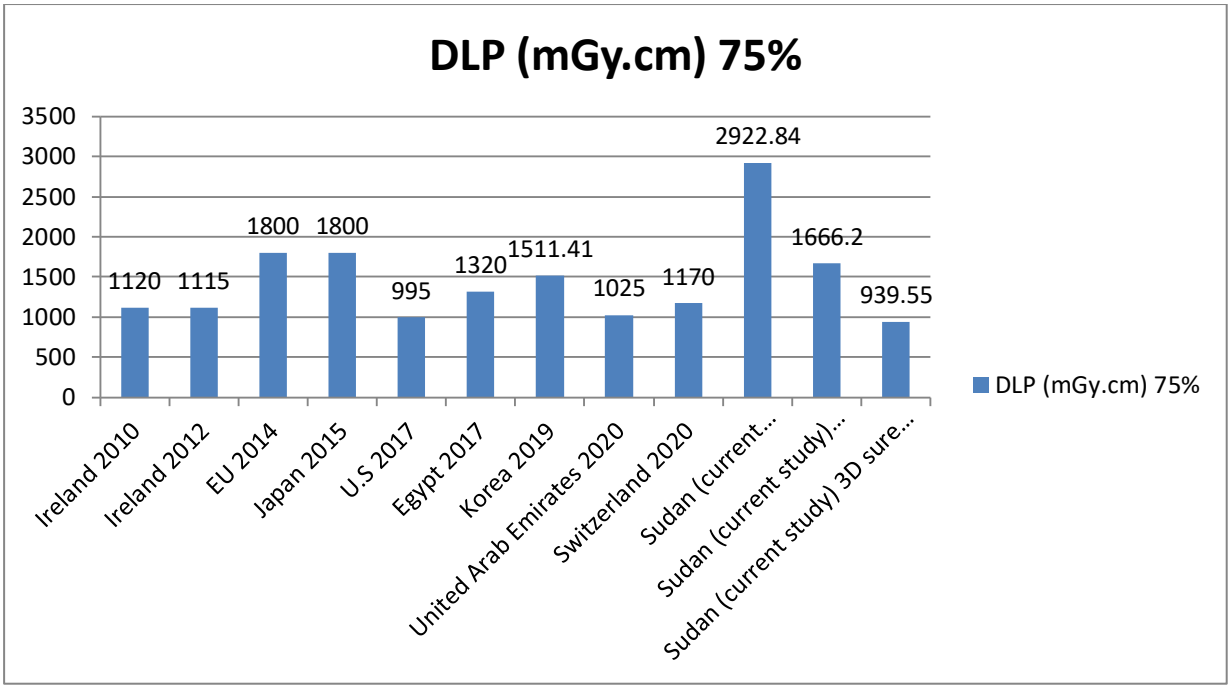

Fig (4.6): show 75% of DLP (mGy.cm) for abdomen multi-phase study in different country and percent study.

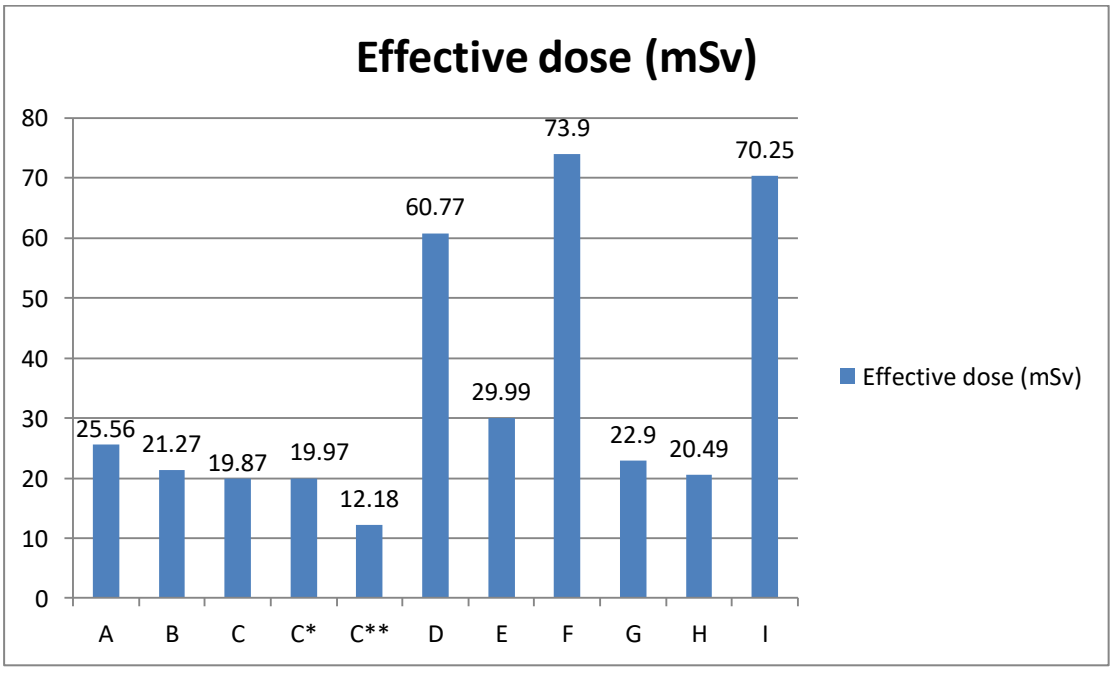

Fig (4.7): show the average effective dose (mSv) for complete tri-phase procedure for adult patient in nine hospitals/diagnostic centers.

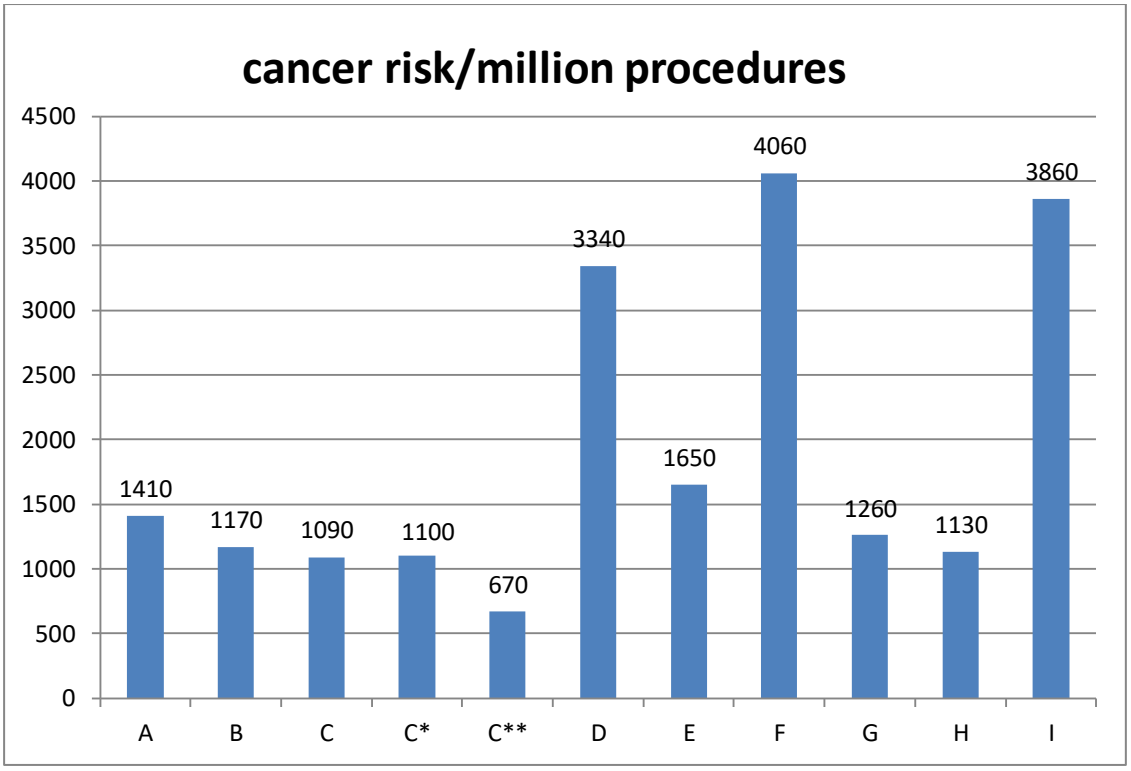

Fig (4.8): show the number of expected cancer incidence per million procedures of complete multi-phase of abdominal CT examination.

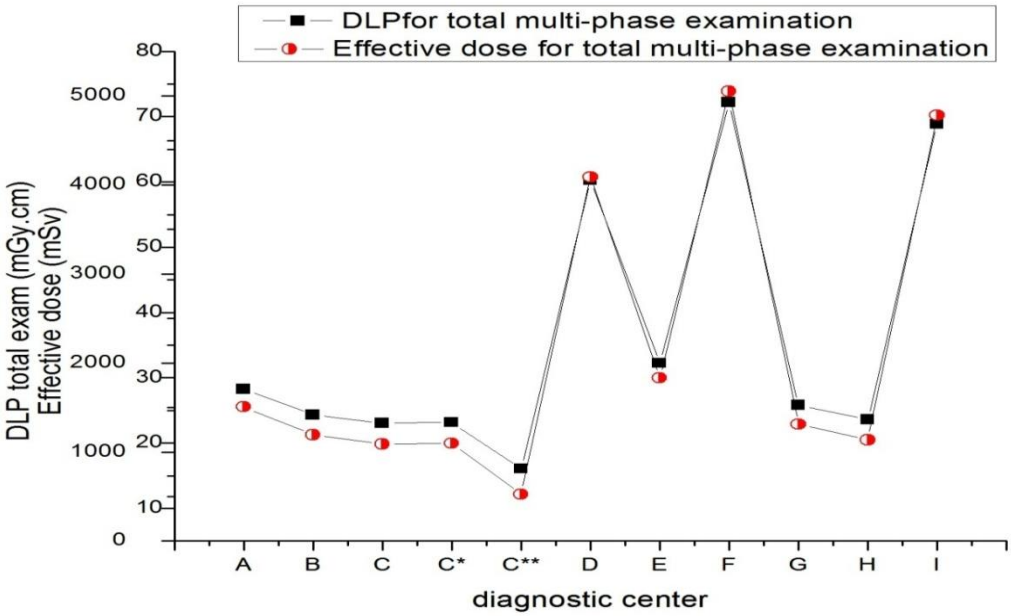

Fig (4.9): show the mean DLP (mGy.cm) and the mean effective dose (mSv) for adult patient in nine hospitals/diagnostic centers

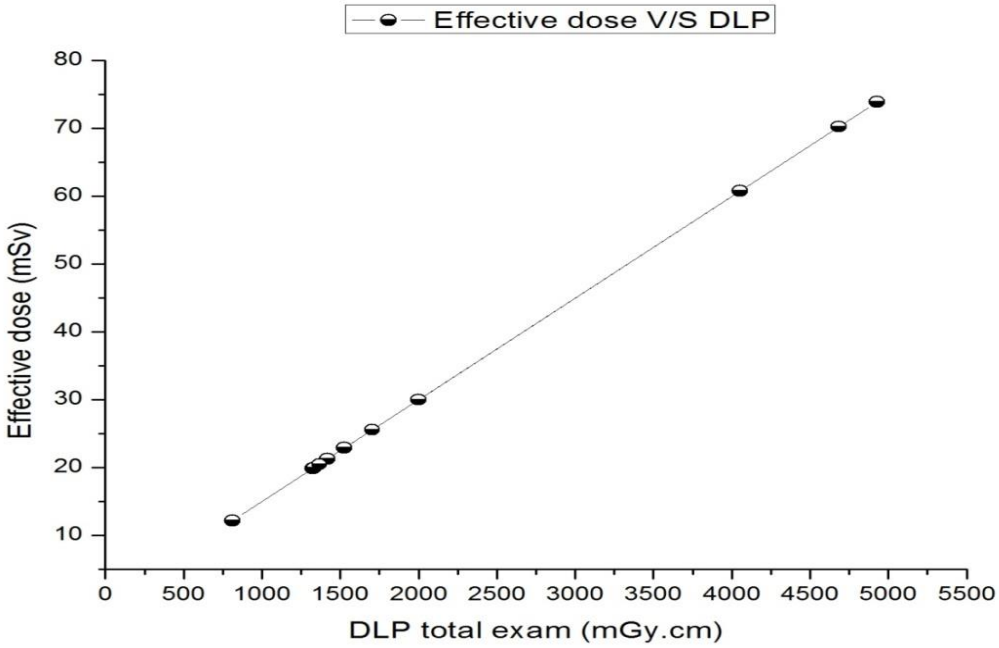

Fig (4.10): show the relationship between the mean DLP (mGy.cm) and the mean effective dose (mSv) for adult patient in nine hospitals/diagnostic centers

4.4 Image quality analysis:

Table 4.10 shows mean density (HU) in rejoins of interest (ROIs) for Lung, Liver and Bone and their standard deviations (SD) and SNR (HU/SD) in four hospitals.

DC / hospital code	Lung		Liver		Bone	
	HU ± SD	SNR (HU/SD)	HU ± SD	SNR (HU/SD)	HU ± SD	SNR (HU/SD)
B	-755.68±23.66	31.93	68.33 ± 11.92	5.73	337.25±49.16	6.86
C	-737.68±39.22	18.81	63.88 ± 20.02	3.19	436.84±65.12	6.71
C*	-788.16±28.86	27.31	73.15 ± 14.58	5.02	361.37±42.59	8.49
C**	-765.28±37.79	20.25	81.22 ± 18.22	4.38	378.19±43.91	8.61
E	-767.47±24.62	31.18	56.72 ± 17.41	3.25	350.02±44.87	7.8
H	-748.96±29.48	25.41	73.8 ± 21.47	3.44	346.82±48.86	7.1

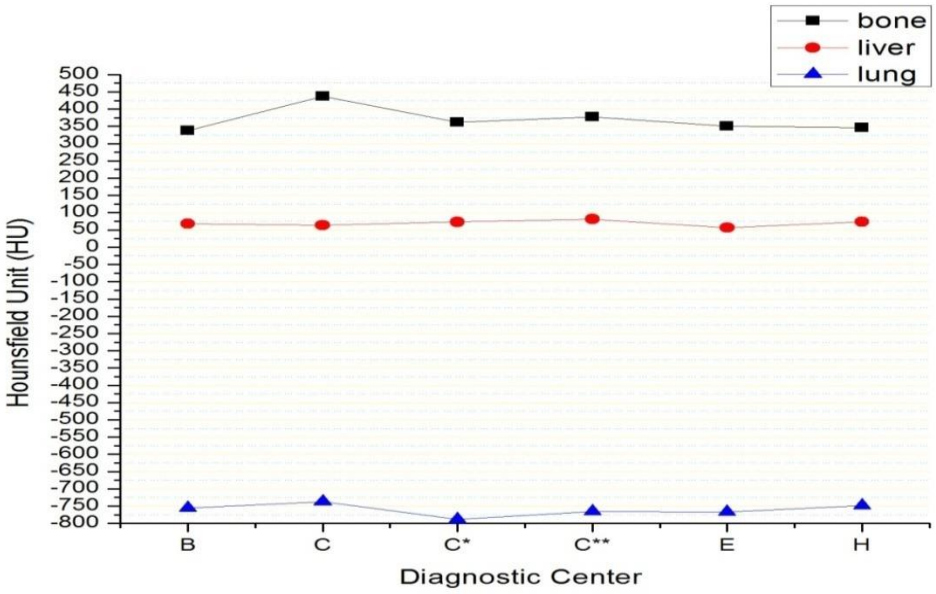

Fig (4.11): show mean Hounsfield Unit (HU) in Lung, Liver and Bone for adult patient in nine hospitals/diagnostic centers.

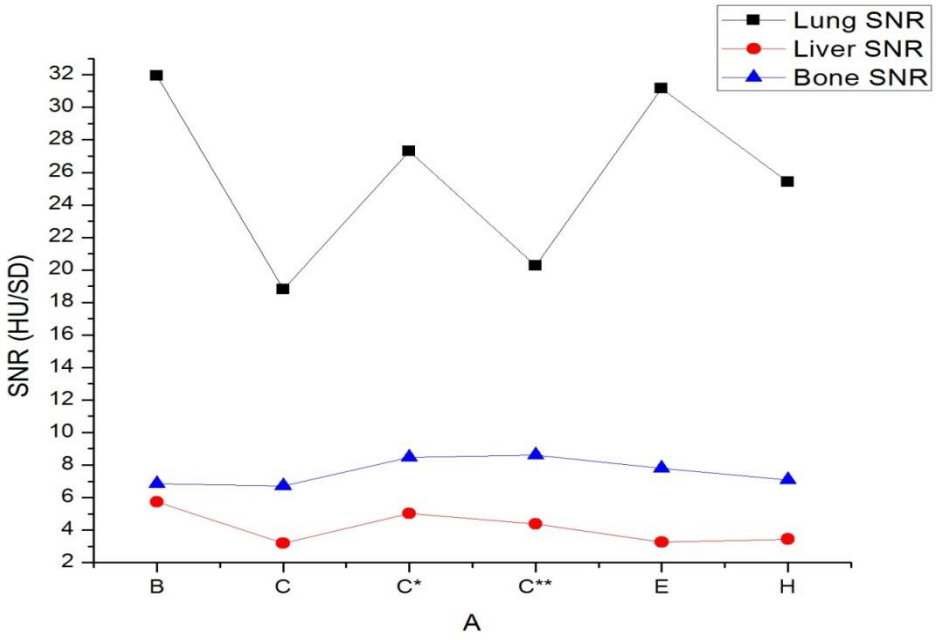

Fig (4.12): show mean Signal to Noise Ratio (HU/SD) in Lung, Liver and Bone for adult patient in nine hospitals/diagnostic centers

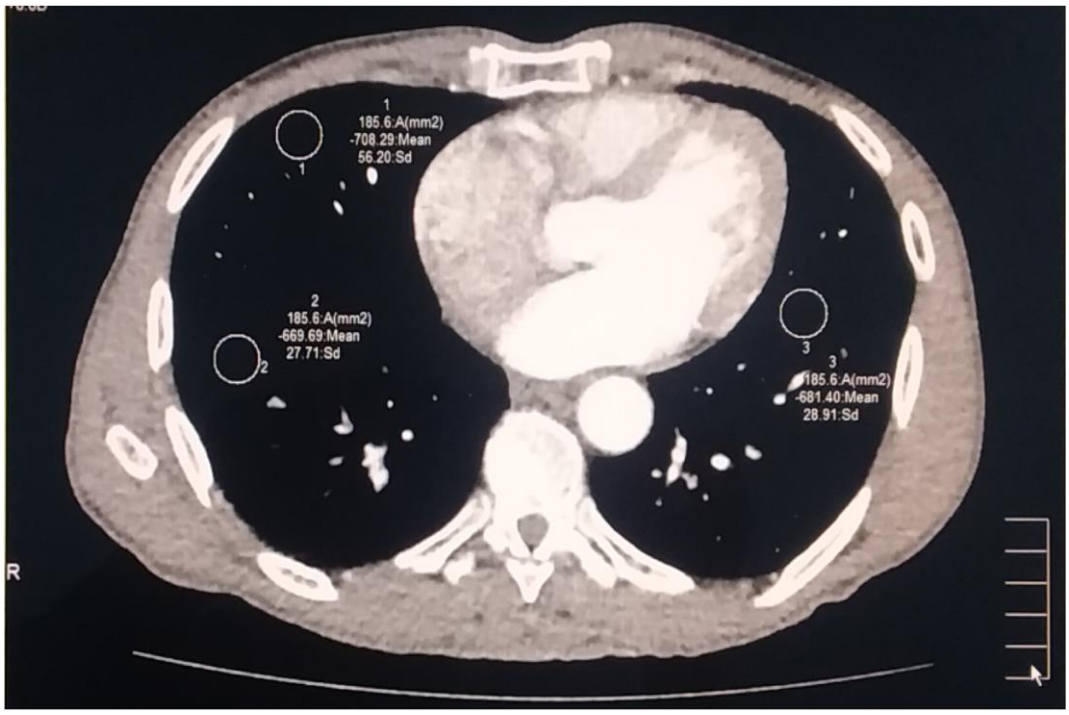

Fig. 4.13. Measurements of noise in CT image for lung during low dose imaging protocols (120 kVp, 40 mAs, rotation time 0.5 s and helical pitch 65).

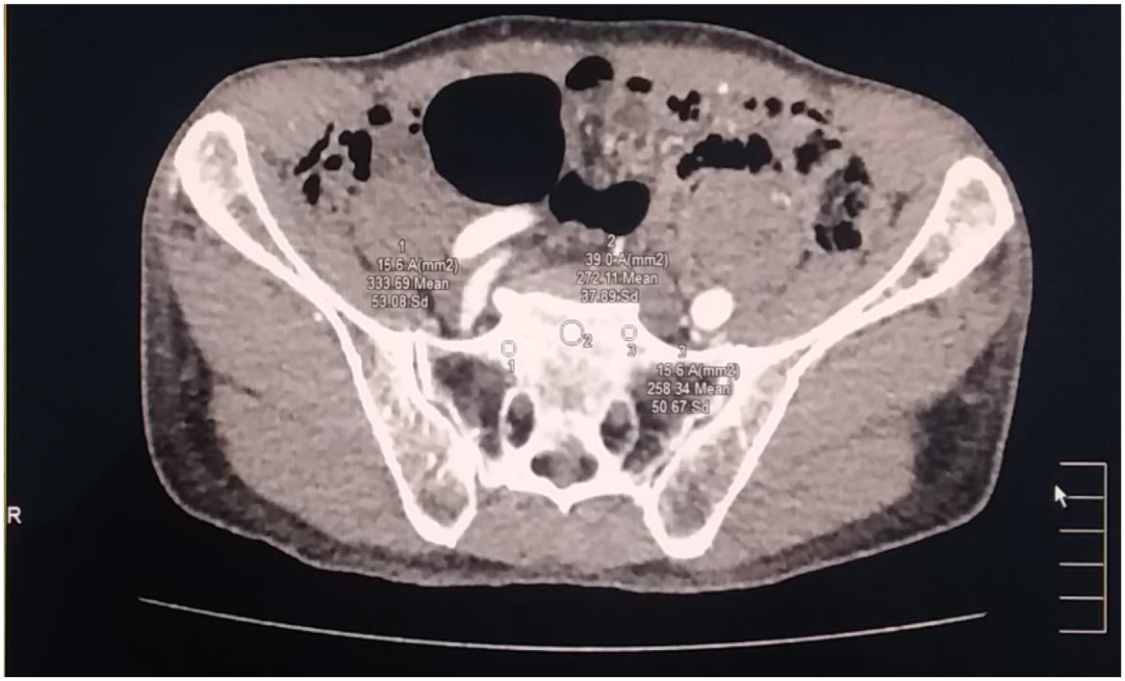

Fig. 4.14. Measurements of noise in CT image for bone during low dose imaging protocols (120 kVp, 40 mAs, rotation time 0.5 s and helical pitch 65).

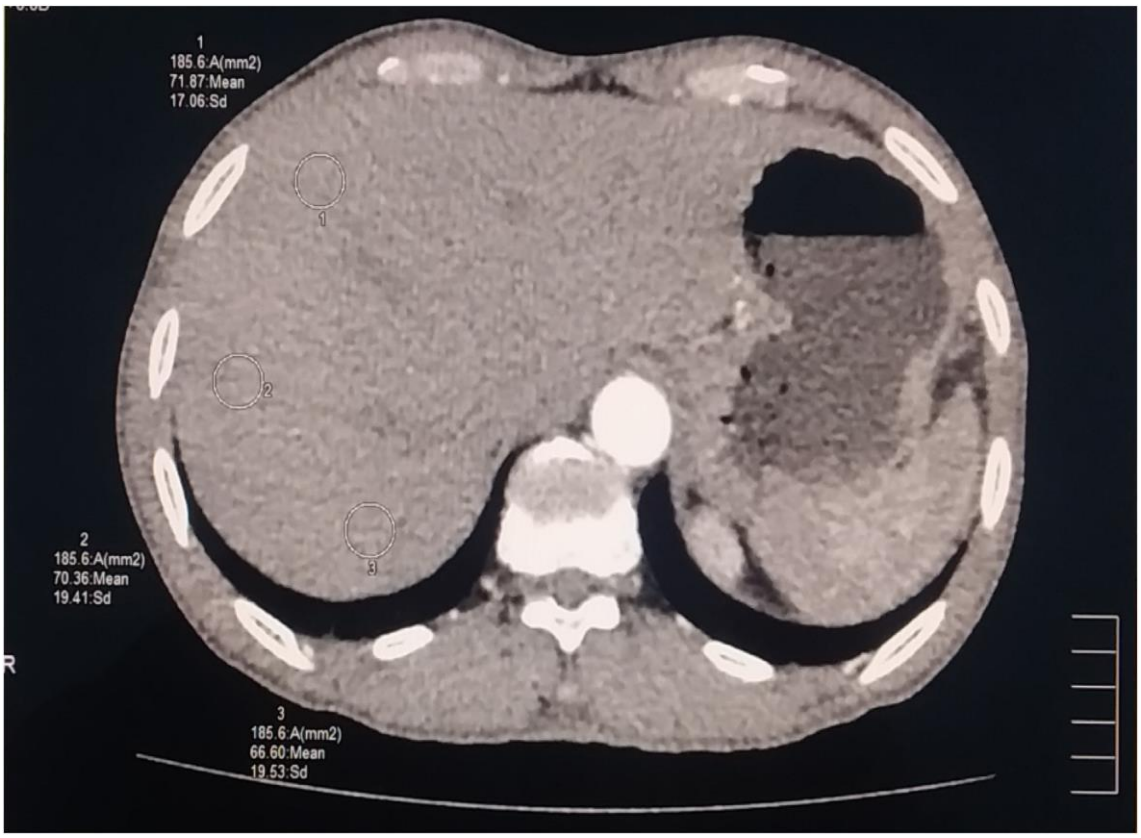

Fig. 4.15. Measurements of noise in CT image for liver during low dose imaging protocols (120 kVp, 40 mAs, rotation time 0.5 s and helical pitch 65).

4.5 Results related to the pediatric patients:

Pediatric patients undergo CT examination requires special consideration, in this study 58 pediatric study composed of 44 (79%) male and 14 (24%) female of pediatric patients undergoing abdomen multi-phase CT scan were studied in 6 out of 9 representative diagnostic centers (table 4.2), which are offering abdomen multi-phase CT examination for pediatric patient.

4.6.1 Radiation dose parameters:

Table 4.11 present the results of CTDIvol for pediatric patients' in six hospitals.

DC code	CTDIvol mGy (Mean ± SD)	Range (Min – Max)	1st Quartile (Q1)	3rd Quartile (Q3)	Interquartile Range (Q3 - Q1)
A	3.16 ± 0.86	(2.69 – 4.89)	2.69	3.75	1.06
B	3.16 ± 0.75	(2.51 – 3.98)	2.63	3.98	1.35
C	5.76 ± 2.77	(1.27 – 8.48)	5.3	7.32	2.02
E	6.8 ± 5.02	(2.18 – 11.2)	2.44	11.16	8.72
F	16.16 ± 7.91	(10.3 – 29.55)	10.3	16.05	5.75
G	5.84 ± 3.16	(3.24 – 9.35)	3.24	9.35	6.11
Total	6.81±3.41	(1.27 – 29.55)	4.03	8.6	2.19

Table 4.12 present the results of DLP of complete procedure for pediatric patient in six hospitals.

DC code	DLP mGy.cm (Mean ± SD)	Range (Min – Max)	1st Quartile (Q1)	3rd Quartile (Q3)	Interquartile Range (Q3 - Q1)
A	485.3 ± 191.32	(330.04–845.32)	353.68	649.96	296.28
B	373.16 ± 20.53	(343.11–399.74)	369.16	380.88	11.72
C	716.56 ± 364.67	(121.1 – 994.4)	614	952.9	338.9
E	1119.68 ± 849.36	(398.7 – 2109.4)	411.65	1827.7	1416.05
F	3347.86 ± 2061.58	(1672.8–6726.6)	1858.3	3759	1900.7
G	1308.33 ± 542.3	(841 – 1908)	841	1908	1067
Total	1225.15± 671.63	(121.1–6726.6)	741.3	1579.74	838.44

Table 4.13 present the results of DLP of single phase for pediatric patient in six hospitals.

DC code	DLP mGy.cm (Mean ± SD)	Range (Min – Max)	1st Quartile (Q1)	3rd Quartile (Q3)	Interquartile Range (Q3 - Q1)
A	112.13 ± 37.15	(82.51– 169.06)	88.42	162.49	74.07
B	105.23 ± 13.63	(92.29 –124.31)	95.22	114.37	19.15
C	156.91 ± 68.57	(40.37 –204.67)	150.07	198.88	48.81
E	248.57 ± 180.6	(79.74 –421.88)	92.95	404.19	311.25
G	309.48 ± 145.9	(210.25 – 477)	210.25	477	266.75
Total	261.22±121.49	(40.37 –121.49)	183.58	330.57	146.99

4.5.2 Effective dose and cancer risk:

Table 4.14 present the results of effective dose and cancer risk of complete procedure for pediatric patient in six hospitals.

DC code	DLP mGy.cm Complete examination	Effective dose (mSv)
A	485.3	7.28
B	373.16	5.60
C	716.56	10.75
E	1119.68	16.80
F	3347.86	50.22
G	1308.33	19.62
Total	1225.15	18.38

Table 4.15 present the results of effective dose and cancer risk of complete procedure for different age group of pediatric patient in six hospitals.

Age group	DC code	CTDIvol mGy (Mean)	DLPsingle phase mGy.cm (Mean)	DLPtotal mGy.cm (Mean)	Effective dose (mSv)	Cancer risks per procedure *10-5
1 to 5 years	B	3.98	119.34	358.02	10.74	59.07
	C	1.27	40.37	121.1	3.63	19.98
	E	6.69	233.12	972.35	29.17	160.44
	F	11.74	475.77	2084.57	62.54	343.95
6 to 10 years	A	2.7	90.67	380.36	7.61	41.84
	B	2.61	95.82	383.26	7.67	42.16
	E	11.12	421.88	2109.4	42.19	232.03
	F	22.8	873.8	5242.8	104.86	576.71
11to15 years	A	4.32	165.78	747.64	11.22	61.68
	C	4.31	185.53	862.65	12.94	71.17
	E	2.7	106.15	424.6	6.37	35.03
	G	5.84	309.48	1308.33	19.62	107.93
1 to 15 years	total	6.67	259.81	1249.59	26.55	146

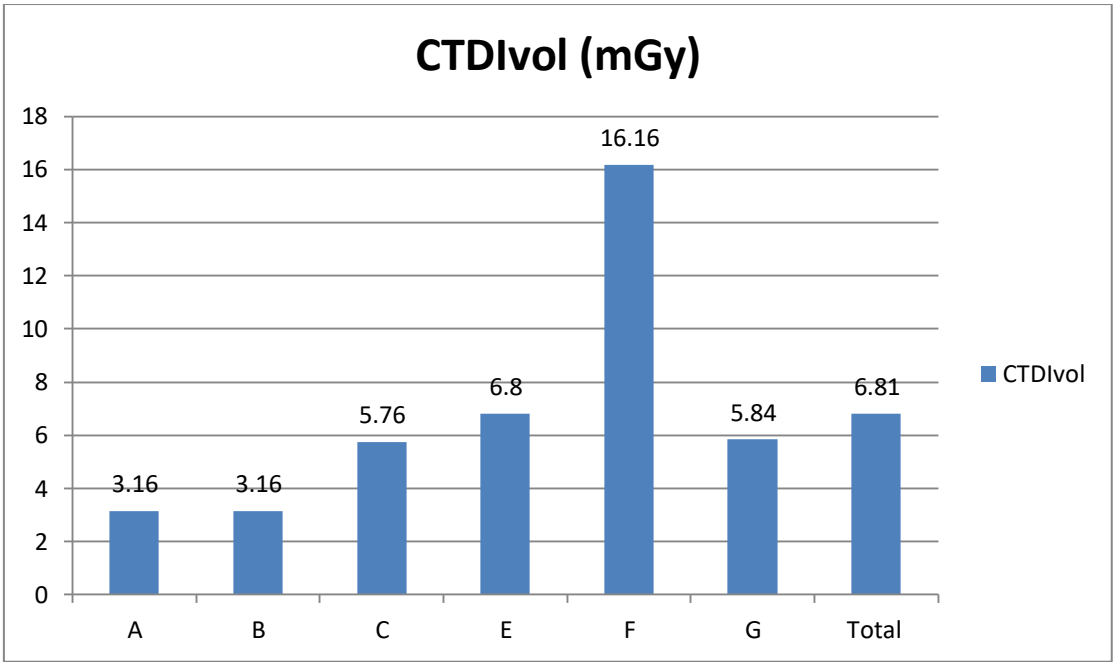

Fig (4.16): show the average CTDIvol (mGy) in pediatric patient for complete multiphase abdomen CT examination in six hospitals.

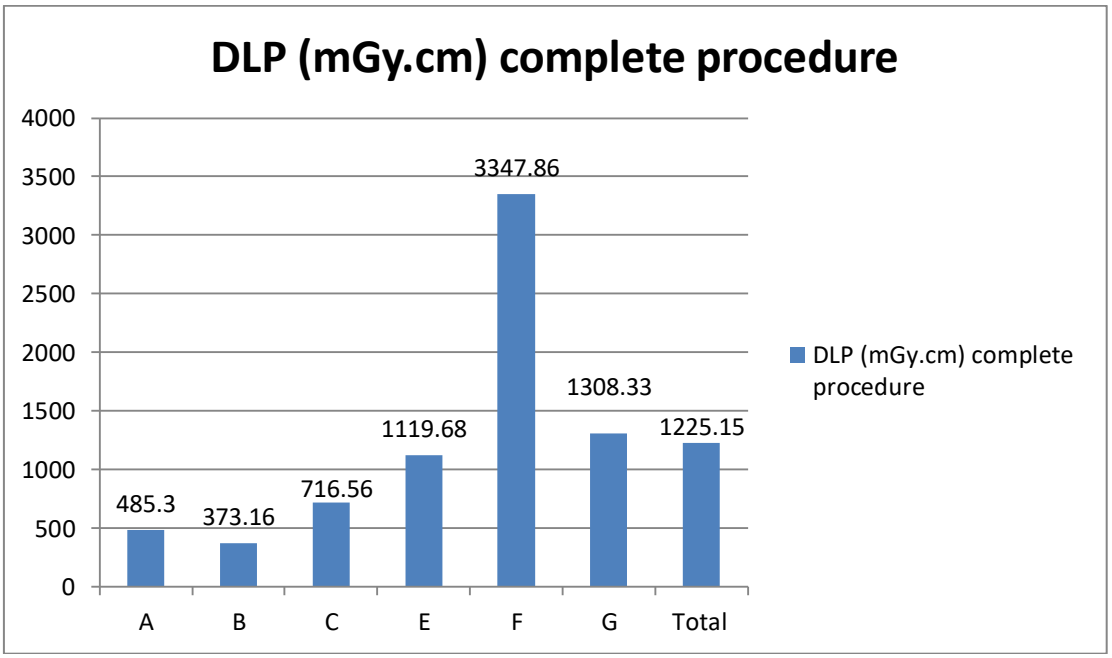

Fig (4.17): show the mean DLP (mGy.cm) in pediatric patient for complete multiphase abdomen CT examination in six hospitals.

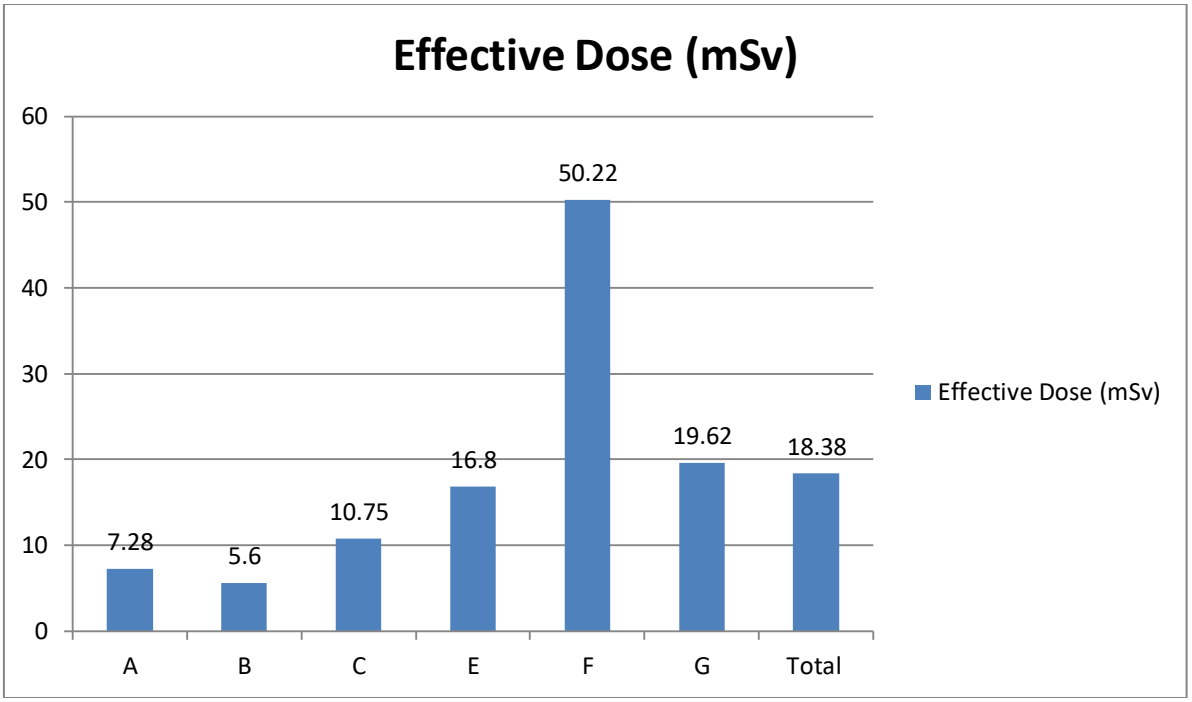

Fig (4.18): show the mean effective dose (mSv) in pediatric patient for complete multiphase abdomen CT examination in six hospitals.

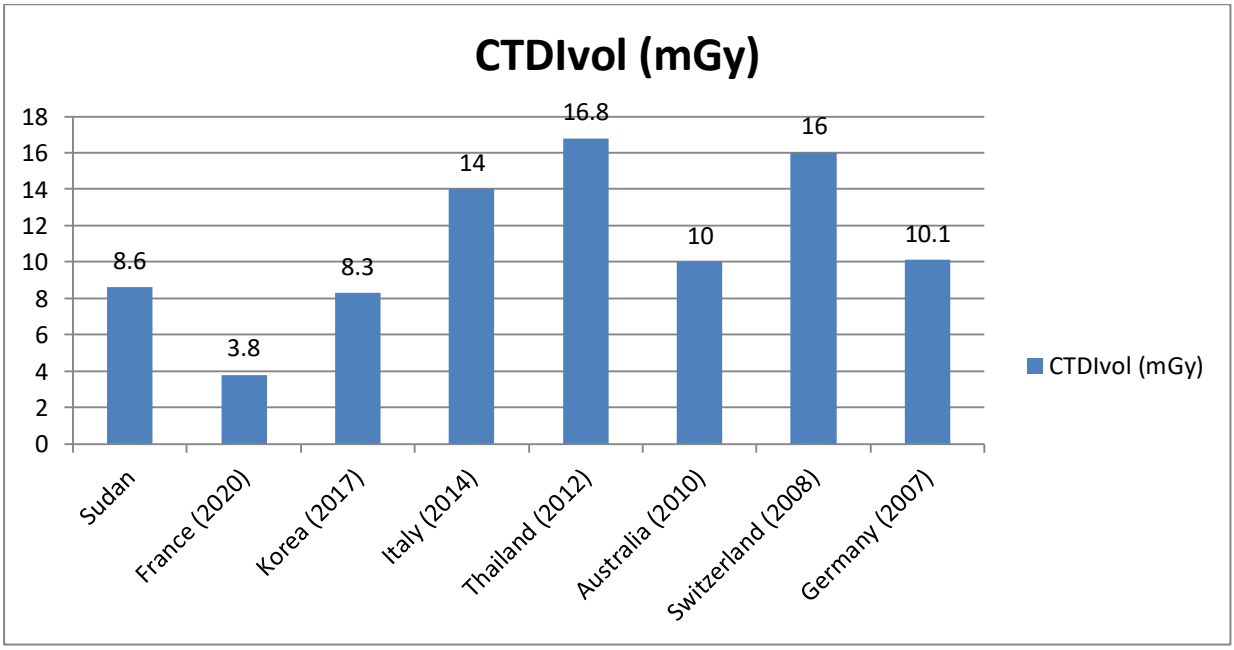

Fig (4.19): show comparisons of mean CTDIvol(mGy) of previous studies with current study.

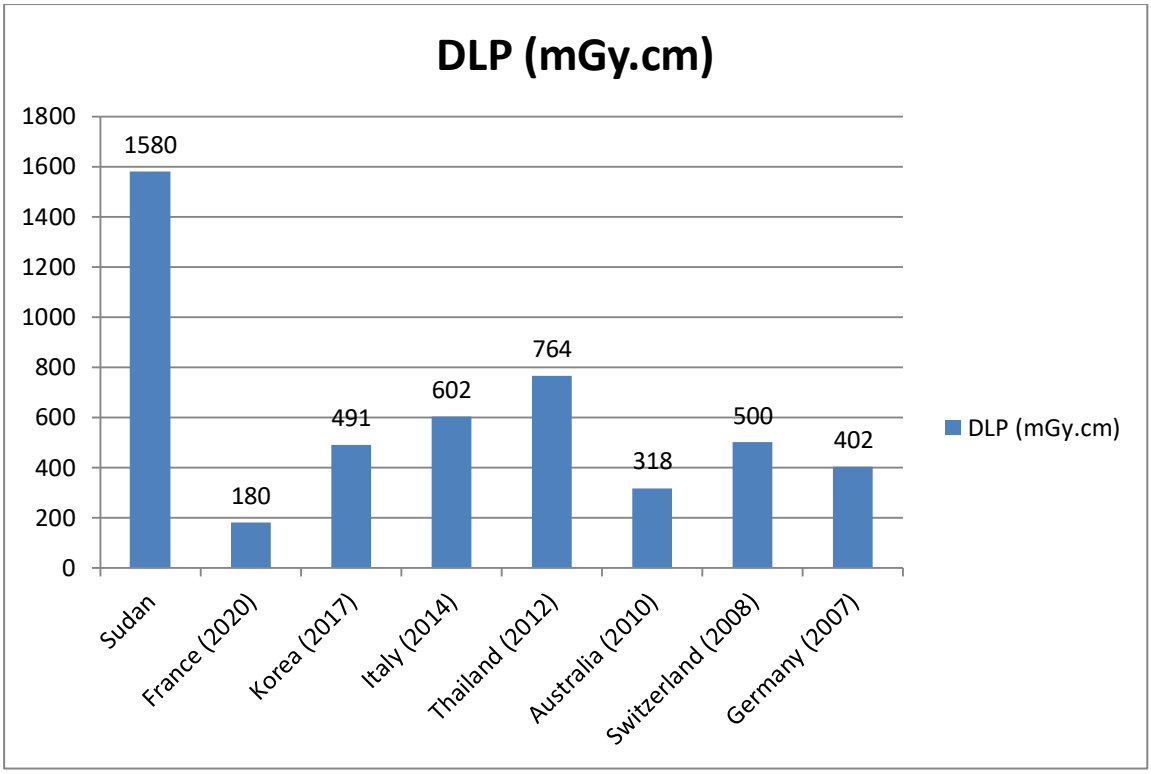

Fig (4.20): show comparisons of mean DLP (mGy.cm) of previous studies with current study.

CHAPTER FIVE

DISCUSSIONS, CONCLUSION and RECOMMENDATIONS

CHAPTER FIVE

DISCUSSIONS, CONCLUSION and RECOMMENDATIONS

5.1 Discussions:

The challenge of patient protection from exposure to ionizing radiation in medical imaging has been increased after the advancement of MDCT. Advanced technology CT systems (not least, multi detector CT and helical acquisition) have enabled short CT scanning times, reduced amounts of contrast medium and volumetric acquisition, all moving towards more accurate diagnostic capability.

A good fraction of medical procedures have moved from conventional angiography to vascular CT. a worldwide remarkable increase in the annual numbers of CT studies was reported, Nickoloff et al 2001 reported about 33 million CT examinations was conducted in United State in 1998, 13.3 million in 1990 and 3.6 million in 1980. The percentage of increasing in annual numbers of CT examinations in United State from 1980 to 1998 is about 900%. Today, CT is prominent source of exposure to ionizing radiation as results of continues emerging of wide range of new clinical applications and the feasibility of conducting multi-phase enhancement studies such as CT angiography and CT urography. Vascular CT in particular represents one of the main sources of elevated radiation exposure compared to other CT examinations due to the large area covered and the potential numbers of procedures a patient might go through. The present study has concerned abdominal contrast enhanced multi-phase CT procedures for both adult and pediatric patients to provide a better understanding of current practice, apply low dose protocol, propose diagnostic reference level and optimize image quality and radiation dose.

CT dose parameters were estimated in term of CTDIvol mGy and DLP mGy.cm by using three different protocols for patients undergoing contrast enhanced multi-phase abdominal CT examination.

Table 4.4 present the mean values of CTDIvol (mGy) and it is first and third quartile for standard dose protocol (current practice) in nine hospitals. The overall mean CTDIvol was 12.88 ± 2.75 mGy ranging from 3.3 to 28.18, wide variations in dose values for patients in different hospitals were observed, the variation attributed to differences in patient size and BMI (except in hospital (D) a fixed dose value was observed in different patient size), this range is within acceptable reference dose of CT accreditation reported by ICRP 87 for adult in CT for routine abdomen, European guideline on quality criteria for computed tomography EUR16262, American association of physicist in medicine (AAPM, 2011) and American College of Radiology (ACR 2008). In some hospitals such as B, C, G and H a comparable dose value were observed, these findings illustrate no significant variations in doses values of patients due to use of different CT facilities, so it was indicates there is a high need of dose optimizations of these facilities (fig 4.1).

Table 4.5 and 4.6 presents the mean values of DLP mGy.cm and it is first and third quartile for standard dose protocol (current practice) in nine hospitals. The overall mean value of DLP for complete multiphase abdominal procedure was 2555.4 ± 873.57 mGy.cm ranging from 257 to 9263.5 mGy.cm. a wide variations in DLP were observed, the lowest value of DLP was found in diagnostic center (C) and the highest value of DLP was found in diagnostic center (F) which is about 3.7 times of the lowest DLP, the variations were also observed in the same hospital, this variations attributed to variations in scan length, tube current, patients size and body mass index (BMI) and the total number of phases (4-6 phase) during complete multi-phase abdominal CT procedure, comparable dose value were observed in hospitals B, C, G and H and

the elevated dose value were observed in hospitals D, F and I Fig (4.2). The overall mean value of DLP for single phase of abdomen was 626.1± 183.7 mGy.cm having range of 65.3 – 2193.7 mGy.cm, the upper value of DLP for single phase in hospital D is about 65% higher than acceptable reference dose of routine abdomen CT reported by ICRP 87and EUR16262. The mean value of DLP for single phase in hospital H and I is about 1.5 time reference dose reported by ICRP 87 and EUR16262. These findings illustrate to high need of dose optimization.

Diagnostic reference level (DRLs) for participated hospitals were calculated and presented in tables (4.4 & 4.5) the resultant values of 75% of DLP (mGy.cm) of current study was compared to DRLs of multi-phase abdomen CT studies reported in different countries in the region and worldwide, from the survey (Table 2.1), the highest 3rd quartile values of DLP were found in Japan (2015) and in EU (2014) and the lowest value was found in the U.S (2017). In comparing the 3rd quartile values of CTDIvol and DLP of standard dose protocol of current study with the 3rd quartile values obtained from the literature review of previous study in the region and in the worldwide, the 3rd quartile values of CTDIvol in standard dose protocol of the current study was comparable to the reported values of CTDIvol in EU.2014 and Japan 2015 and 2020, these findings indicate for acceptable dose per slice received by patients. The 3rd quartile value of DLP obtained by standard protocol of current study was about three fold greater than that of U.S and about 30% to 40% greater than values of EU 2014 and Japan 2015 and Japan 2020. These findings illustrate patients received an avoidable radiation dose, attributed to variation in mAs, KVp, Scan time, scan length and number of phases, therefore, accurate optimization of imaging parameters with limited number of phases for answering the requested diagnostic task is highly recommended.

In use of sure exposure low dose technique in state of standard dose protocol in

hospital (C), a reduction of about 50% in patients radiation dose per slice (CTDIvol) was observed, and reduction in CTDIvol of about 60% in comparing with that of EU 2014 and Japan 2015 was observed, these reduction in CTDIvol attributed to advanced adaptive iterative dose reduction technology, reduced mAs and surprised desired image quality (Table 4.8). Sure exposure low dose technique provides lowest radiation exposure to the patients during complete abdomen multi-phase CT examination, sure exposure low dose technique provide dose reduction of about 39% when it was compared to standard dose protocol in hospital C. which it presented as the lowest exposure of radiation dose to patient when it was compared to other hospitals included in this study, also same value of dose reduction was obtained when sure exposure dose value compared to combination dose value. Also sure exposure low dose technique provides about 83.5 % of reduction in patient dose when it was compared to highest radiation dose obtained by using standard protocol in hospital F (Fig 4.2). Also sure exposure low dose protocol provides overall dose reduction of about 68% when it was compared to standard dose technique. The 3rd quartile value of DLP was about 68% lower than that obtained by the standard protocol of the current study and it was about half of DRLs of EU (2014) and Japan (2015). Sure exposure low dose technique secure long lifetime of tube generator of CT device and provide minimum radiation exposure to patients (Table 4.8 & Fig 4.5).

In use of combination of low dose protocol with standard dose or high quality dose protocol in hospital C, the resultant value of CTDIvol is comparable to that value of CTDIvol obtained by standard dose protocol (Table 4.4 & 4.8). But the value of DLP obtained by using combination protocol is lower than DLP values of EU 2014 and Japan 2015 and higher than of the other counties (Table 4.8) & (Fig 4.5 & 4.6).

The overall mean value of effective dose for standard protocol was 38.33 mSv,

in some cases highly elevated effective dose above 100 mSv was observed (Table 4.5), which is controversy dose for cancer mortality. In use of combination of standard dose protocol with high quality or low dose protocol the mean effective dose was 19.97mSv, and for sure exposure low dose technique it was 12.18 mSv, which is lower by up to 68% of the effective doe of standard dose protocol (Table: 4.9 & Fig: 4.7). Cancer risk per procedure was estimated, the overall expected mean value of cancer risk per procedure were 2110 (1090 – 4060) , 1100 and 670 cancer case pre million procedures for standard dose protocol, combination of standard dose with low dose or high quality dose protocol and sure 3D low dose protocol respectively (Table: 4.9 & Fig:4.8). Standard dose protocol provides high risk value of expected patient's cancer mortality, while low dose protocol provides the least risk. Consequently, several radiosensitive organs such as breast, gonads and ovaries may have higher risk for cancer mortality. Although, the estimated cancer risk value can be restricted by low dose cancer risk uncertainties due to long latent periods of cancer appearance, which is may takes several years up to decades (Alkhorayef et al., 2021). Therefore, CT was classified as a dominant contributor to the resultant amount of effective dose estimated from medical imaging procedure. Fazel et al., reported that about 75% of medical radiation exposure have been obtained from CT examination. While, the frequency of CT examinations is just about 11% compared with another imaging modalities (Fazel et al., 2009). Although, proper justification of imaging procedures and optimization of imaging protocols helps in prevention of patients from unproductive exposure of ionizing radiation. In addition, the use of alternative dose reduction tools offered by different CT manufactures will prevent the patients from over exposure of radiation dose. Unfortunately, many centers do not take the advantage of the dose reduction capabilities of their scanners, because of a lack of familiarity and understanding as to how these tools work. Herein, by

applying sure exposure low dose technique in hospital C a reduction in dose of about 39% was achieved. For some vascular CT procedures effective measures have already been reported in obtaining dose reduction, including tube voltage reduction by 20 kVp and vendor optimization protocols, reducing the dose by up to 30% and 80% respectively (Liu and Platt, 2014; Schindera et al., 2009). It is important to note that reduction of tube voltage is available in all recent CT modality machines (64 and 128 detectors). Thus increased operator awareness towards radiation dose and expected risk may help in implementation of safety culture in CT departments. One remaining basic challenge in vascular CT is the absence of any standard injection protocol (Liu and Platt, 2014), thus optimisation remains a continuing issue for radiation protection personnel. Staff training in radiation protection and dose optimization is recommended.

A special concern for pediatric patient is recommended; dramatically increase in pediatric CT has been reported, it was estimated that pediatric CT frequency ranges from 6% to 11% in developed countries. The increase in pediatric procedures may be attributed to the introduction of faster scanners, which reduce the need for sedation while obtaining diagnosable findings (Mettler et al., 2020; Goske et al., 2008). In pediatric patient, the estimated CTDIvol and DLP (mGy.cm) for different CT vendors was presented in tables (4.11 & 4.12), The overall mean values for CTDIvol (mGy) and DLP (mGy.cm) in pediatric patient were 6.81±3.41and 1225.15±671.63, corresponding to Q^{1st} and Q^{3rd} quartiles of dose values of 4.03, 8.6 mGy and 741.3, 1579.74 mGy.cm for CTDIvol (mGy) and DLP (mGy.cm) respectively (Tables 4.11 and 4.12). Patients dose (DLP (mGy.cm)) is higher compared to the previous reported diagnostic reference levels (DRL) in some countries, France, Switzerland, Thailand, Korea, and Germany, Italy, and Australia (Table 2.2). Fig (4.19) Illustrate the DRL for CT multi phase abdomen in terms of volume CTDI (CTDIvol (mGy)). Significant discrepancies in DRL values among previous

studies ranging from 8.8 to 30 mGy (Matsunaga et al., 2019; Hayton and Wallace, 2016; Varghese et al., 2018; Kim et al., 2015; Santos et al., 2013; Roch and Aubert, 2013; Shrimpton and Wall, 2000). The derived DRL for multiphase CT abdomen comparable with the lowest values reported in the literature (Fig. 4.20). The results showed that the DRL value is decreasing gradually from 2000 till 2021, with some exceptions. Technological advancement of CT machines and in-crease the operators awareness are factors that may contributed in dose reduction. Therefore, according to the ICRP recommendations, DRL should be reviewed every three to five years (ICRP, 2017). Pediatric results indicate to the use of high CT imaging protocol to perform pediatric study, operators tend to use high exposure parameters to obtain very high image quality (high-resolution CT). Also, all pediatric patients underwent three phasic abdominal CT procedures. Although the dose per slice (CTDIvol (mGy) is comparable with previous studies, the DLP (mGy.cm) is greater than values reported previously due to the increase in the scan length and multiphase CT procedures, which include the pelvic region. It should be noted that the patient radiation dose per single-phase procedure is comparable with the previous studies (Tables 5 and 7). The variation in patients' doses is attributed to variation in the imaging protocols and number of phases performed per pediatric CT abdomen procedure. Patient dose per procedure also showed wide variation in DLP (mGy.cm), while limited variation was detected for CTDIvol (mGy). Thus the variation in scan length and number of phases may be contributing significantly in DLP variations (Table 4.12 & 4.13). The wide variation in patients' dose values amid the previous studies and DRL values highlight the considerable variability of CT abdomen imaging protocols used in the different departments for the same pediatric patients' groups. Previous reported DRL for pediatric CT abdomen data showed that there is no standardized imaging protocol. It is noteworthy to mention that CT dose reduction technology is developing rapidly.

However, the dose is independent of the CT modality or technology, suggesting that the operator skills and imaging protocol are essential in dose reduction. Guite et al. stated that approximately 50% of CT multiphase procedures had an additional one or more unnecessary phases depend on the American College of radiologist (ACR) imaging criteria, with 78% of the procedures without the number of phase indication (Guite et al., 2011; Mez-rich, 2008; Huang et al., 2010). Vassileva et al. (2015) reported that the rate of the multiphase procedure is up to 60% compared to a single-phase (Vassileva et al., 2015). It was stated that pediatric CT abdomen procedures are not adjusted, and children underwent unnecessary multiphase CT imaging procedures (Frush, 2018). Garba et al. (2021), reported variation in patient's doses during CT abdomen and DRLs values due to the variation in scanner technology, imaging protocol. Cooper et al. reported considerable variation in pediatric patient doses in CT abdomen due to variation in weight, age and the number of phase for CT abdomen procedures (Cooper et al., 2017). The radiation risks per procedure are trivial, and the benefit of justified and optimized CT procedures outweigh the projected risks. MRI provides excellent contrast resolution soft-tissue images. Another imaging procedures such as US and MRI that do not encompass exposure to ionizing radiation is recommended whenever possible (Ibrahim et al., 2020; Greenwood et al., 2015).

5.2 Conclusion:

Patient doses during CT abdomen triphasic procedure were evaluated using the standard dose, combination of low dose with standard or high quality dose and low-dose imaging protocols. Wide variations in patient doses indicate patients receive an avoidable radiation exposure. 3D sure exposure low dose protocol provides 40 to 70 % of reduction in dose without compromising the diagnostic image quality. Image quality assessment showed reduction of patient dose to be

possible via noise suppression while reducing the tube current. Training in radiation protection for patients is recommended to prevent unnecessary exposure. Furthermore, adjustment of exposure parameters by qualified medical physicist is recommended to ensure that the patients will receive the minimal dose consistent with clinical indication; any dose reduction will significantly reduce the probability of solid cancer and leukemia risks, especially in pediatric patient. The cancer risk per procedure should be considered during the justification and image acquisition stages. Particular concern should be paid to the number of phases necessary for the accurate diagnosis. Based on the clinical indication and image acquisition must be limited to the area of interest. Patient dose reduction is possible by implementing appropriate referrals criteria, adjusting imaging protocol based on patient weight, the use of dose reduction technique, and staff training on radiation protection culture at the department.

5.3 Recommendations:

Based on the results of the current thesis, the following are recommended

1. Elevated radiation dose have been received by patients examined with standard dose protocol, in some cases effective dose above 100 mSv was observed, therefore, adjustment of imaging parameters according to patient weight, size and BMI is highly recommended.
2. Use of radio protective shields is recommended to protect radiosensitive organs such as breast, gonads and ovaries from the risk of cancer mortality.
3. Proper justification of imaging procedures and appropriate optimization of imaging protocols by qualified medical physicist helps in prevention of patients from unproductive exposure of ionizing radiation.

4. Adjustment of exposure parameters by qualified medical physicist is recommended to ensure that the patients will receive the minimal dose consistent with clinical indication.
5. Particular concern should be paid to the number of phases necessary for the accurate diagnosis.
6. Clinical indication and image acquisition must be limited to the area of interest.
7. Routine review of clinical protocols by team of radiologist, qualified medical physicist and CT technologist is recommended to avoid patient's unnecessary radiation exposure.
8. Cancer risk per procedure should be considered during the justification and image acquisition stages.
9. Staff training on optimization protocol in CT scan to assure that all dose-saving techniques well used to tailor exam protocol.
10. Establish a national diagnostic reference level for CT procedures according to the imaging protocol and the type of the procedure.
11. Special attention should be paid for pediatric patients due to their high sensitivity to ionising radiation.

REFERENCES

References

-	Aberle, C., et al. (2020). "Update of national diagnostic reference levels for adult CT in Switzerland and assessment of radiation dose reduction since 2010." **30**(3): 1690-1700.
-	Abuzaid, M. M., et al. (2020). "Computed tomography radiation doses for common computed tomography examinations: a nationwide dose survey in United Arab Emirates." **11**(1): 1-6.
-	Abuzaid, M. M., et al. (2020). "Toward National CT Diagnostic Reference Levels in the United Arab Emirates: A Multicenter Review of CT Dose Index and Dose Area Product." **190**(3): 243-249.
-	AC09617961, A. (2012). Quality assurance programme for computed tomography: diagnostic an therapy applications, IAEA.
-	arba, I., Zarb, F., McEntee, M.F., Fabri, S.G., 2021. Computed tomography diagnostic reference levels for adult brain, chest and abdominal examinations: a systematic review. Radiography 27 (2), 673–681.
-	Beister, M., et al. (2012). "Iterative reconstruction methods in X-ray CT." Phys Med **28**(2): 94-108.
-	Brenner, D. J. and E. J. J. N. E. J. o. M. Hall (2007). "Computed tomography—an increasing source of radiation exposure." **357**(22): 2277-2284.
-	C´elier, D., Roch, P., Etard, C., et al., 2020. Multicentre survey on patient dose in paediatric imaging and proposal for updated diagnostic reference levels for France. Part 1: computed tomography. Eur. Radiol. 30, 1156–1165, 2020.
-	Cianci, R., et al. (2019). "Ultra-low dose CT colonography with automatic tube current modulation and sinogram-affirmed iterative reconstruction: Effects on radiation exposure and image quality." **20**(1): 321-330.

-	Cierniak, R. (2011). X-ray computed tomography in biomedical engineering. Springer Science & Business Media.
-	Cooper, J.N., Lodwick, D.L., Adler, B., Lee, C., Minneci, P.C., Deans, K.J., 2017. Patient characteristics associated with differences in radiation exposure from pediatric abdomen-pelvis CT scans: a quantile regression analysis. Comput. Biol. Med. 85, 7–12.
-	Elnour, A. M., et al. (2015). "Establishment of Local Diagnostic Reference Level For Brain Ct Procedures." **4**(3).
-	Fazel,R.,Krumholz,H.M.,Wang,Y.,Ross,J.S.,Chen,J.,Ting,H.H.,Shah,N.D., Nasir,K., Einstein,A.J.,Nallamothu,B.,2009.Exposuretolow-doseionizingradiationfrom medicalimagingprocedures.N.Engl.J.Med.361,849.
-	Feigal D. W., Jr (2002). FDA public health notification: reducing radiation risk from computed tomography for pediatric and small adult patients. International journal of trauma nursing, 8(1), 1–2. https://doi.org/10.1067/mtn.2002.121511
-	Feinendegen, L. E., & Cuttler, J. M. (2018). Biological effects from low doses and dose rates of ionizing radiation: science in the service of protecting humans, a synopsis. *Health physics*, *114*(6), 623-626.
-	Foley, S. J., et al. (2012). "Establishment of CT diagnostic reference levels in Ireland." **85**(1018): 1390-1397.
-	Food and Drug Administration (FDA), 2017. What are the Radiation Risks from CT? Available at: https://www.fda.gov/radiation-emitting-products/medical-x-ray-imaging/what-are-radiation-risks-ct, Accessed date: 1 August 2021.
-	Frush, D.P., 2018. “Here”s looking at you, kid’ ... again? Revisiting multiphase CT in children. Pediatr. Radiol. 48 (12), 1711–1713.

-	Galanski, M., Nagal, H.D., Stamm, G., 2007. Pediatric CT exposure practice in the Federal Republic of Germany. Results of a nationwide survey in 2005/6. Medizinishe Hochschule Hannover. http://www.mh hannover.de/fileadmin/kliniken/diagnostische_radiologie/download /Report_German_Paed-CT-Survey_2005_06.pdf. Accessed 27 Jan 2021.
-	Geleijns, J. and R. Irwan (2012). Practical approaches to dose reduction: Toshiba perspective. Radiation Dose from Multidetector CT, Springer**:** 633-645.
-	Goldman, L. W. J. J. o. n. m. t. (2007). "Principles of CT: radiation dose and image quality." **35**(4): 213-225.
-	Goske, M.J., Applegate, K.E., Boylan, J., et al., 2008. The 'Image Gently' campaign: increasing CT radiation dose awareness through a national education and awareness program. Pediatr. Radiol. 38, 265–269
-	Granata, C., Origgi, D., Palorini, F., Matranga, D., & Salerno, S. (2015). Radiation dose from multidetector CT studies in children: results from the first Italian nationwide survey. Pediatric radiology, 45, 695-705.
-	Gregory, K. J., et al. (2009). "Uncertainties in effective dose estimates of adult CT head scans: The effect of head size." **36**(9Part1): 4121-4125.
-	Guite, K.M., Hinshaw, J.L., Ranallo, F.N., Lindstrom, M.J., Lee, F.T., 2011. Ionizing radiation in abdominal CT: unindicated multiphase scans are an important source of medically unnecessary exposure. J. Am. Coll. Radiol. 8 (11), 756–761.
-	Hathcock, J. T. and R. L. J. V. C. o. N. A. S. A. P. Stickle (1993). "Principles and concepts of computed tomography." **23**(2): 399-415.
-	Hayton, A., Wallace, A., 2016 Sep. Derivation of Australian diagnostic reference levels for paediatric multi detector computed tomography. Australas. Phys. Eng. Sci. Med. 39 (3), 615–626.

-	Herman, G. T. (2009). Fundamentals of computerized tomography: image reconstruction from projections, Springer Science & Business Media.
-	Huang, B., Li, J., Law, M.W., Zhang, J., Shen, Y., Khong, P.L., 2010. Radiation dose and cancer risk in retrospectively and prospectively ECG-gated coronary angiography using 64-slice multidetector CT. Br. J. Radiol. 83 (986), 152–158
-	Ibrahim, A., Wales, P.W., Aquino, M.R., Chavhan, G.B., 2020. CT and MRI findings in pancreatic trauma in children and correlation with outcome. Pediatr. Radiol. 50 (7), 943–952.
-	Jessen, K. A., Panzer, W., Shrimpton, P. C., Bongartzm, G., Geleijns, J., Golding, S., ... & Tosi, G. (2000). EUR 16262: European guidelines on quality criteria for computed tomography. *Luxembourg: Office for Official Publications of the European Communities*.
-	Jiang, H. (2009). Computed tomography: principles, design, artifacts, and recent advances. SPIE.
-	Kalender, W. A. J. P. i. M. and Biology (2006). "X-ray computed tomography." **51**(13): R29.
-	Kanal, K. M., et al. (2017). "U.S. Diagnostic Reference Levels and Achievable Doses for 10 Adult CT Examinations." Radiology **284**(1): 120-133.
-	Kanda, R., et al. (2020). "Developing diagnostic reference levels in Japan." Japanese Journal of Radiology.
-	Kim, Han, D.K., Nam, Y.C., Kim, Y.M., Yoon, J., 2015. Patient dose for computed tomography examination: dose reference levels and effective doses based on a national survey of 2013 in Korea. Radiat. Protect. Dosim. 164 (3), 383e91.

-	Kim, J. S., et al. (2019). "National diagnostic reference levels and achievable doses for 13 adult CT protocols and a paediatric head CT protocol: National Survey of Korean hospitals." **187**(2): 220-229.
-	Kim, M., Chang, K., Hwang, J., Nam, Y., Han, D., Yoon, J., 2017. Radiation dose for pediatric and young adult CT: a survey to establish age-based reference levels of 2015–2016 in Korea. Radiat. Protect. Dosim. 175 (2), 228–237.
-	Kritsaneepaiboon, S., Trinavarat, P., & Visrutaratna, P. (2012). Survey of pediatric MDCT radiation dose from university hospitals in Thailand: a preliminary for national dose survey. Acta radiologica, 53(7), 820-826.
-	Lieberman, K., et al. (2002). How should X-ray techniques be modified for pediatric patients in head CT? Radiology, RADIOLOGICAL SOC NORTH AMERICA 820 JORIE BLVD, OAK BROOK, IL 60523 USA.
-	Lin E. C. (2010). Radiation risk from medical imaging. Mayo Clinic proceedings, 85(12), 1142–1146. https://doi.org/10.4065/mcp.2010.0260
-	Liu, P. S. and J. F. J. A. i. Platt (2014). "CT angiography in the abdomen: a pictorial review and update." **39**(1): 196-214.
-	Marchal, G., et al. (2005). Multidetector-row computed tomography: scanning and contrast protocols, Springer Science & Business Media.
-	Matsunaga, Y., Chida, K., Kondo, Y., et al., 2019. Diagnostic reference levels and achievable doses for common computed tomography examinations: results from the Japanese nationwide dose survey. Br. J. Radiol. 92 (1094), 20180290.
-	McCollough, C. H., et al. (2006). "CT dose reduction and dose management tools: overview of available options." **26**(2): 503-512.
-	McCollough, C. H., et al. (2009). "Strategies for reducing radiation dose in CT." **47**(1): 27-40.

-	Mello-Amoedo, C. D. d., et al. (2018). "Comparison of radiation dose and image quality of abdominopelvic CT using iterative (AIDR 3D) and conventional reconstructions." **210**(1): 127-133.
-	Mettler, F.A., Mahesh, M., Bhargavan-Chatfield, M., et al., 2020. Patient exposure from radiologic and nuclear medicine procedures in the United States: procedure volume and effective dose for the period 2006–2016. Radiology 295 (2), 418–427, 192256
-	Nakamoto, A., et al. (2018). "Reduction of the radiation dose and the amount of contrast material in hepatic dynamic CT using low tube voltage and adaptive iterative dose reduction 3-dimensional." **97**(34).
-	Pearce, M. S., et al. (2012). "Radiation exposure from CT scans in childhood and subsequent risk of leukaemia and brain tumours: a retrospective cohort study." **380**(9840): 499-505.
-	Podgoršak, E. B. (2006). "Radiation physics for medical physicists."
-	Protection, I. C. o. R. (1996). Radiological Protection and Safety in Medicine: A Report of a Task Group of Committee 2 of the International Commission on Radiological Protection, International Commission.
-	Quinn, B. M., et al. (2020). "Patient-adapted organ absorbed dose and effective dose estimates in pediatric 18F-FDG positron emission tomography/computed tomography studies." **20**(1): 9.
-	Qurashi, A. A., et al. (2019). "The impact of obesity on abdominal CT radiation dose and image quality." **185**(1): 17-26.
-	Raman, S. P., et al. (2013). "CT dose reduction applications: available tools on the latest generation of CT scanners." J Am Coll Radiol **10**(1): 37-41.
-	Raupach, R. (2012). SAFIRE: Sinogram Affirmed Iterative Reconstruction.
-	Rehani, M. M., Bongartz, G., Golding, S. J., Gordon, L., Kalender, K., Murakami, T., & Wei, K. (2001). International Commission on

	Radiological Protection (ICRP). Publication 87, Managing Patient Dose in Computed Tomography. *Annals of the ICRP*, *30*(4).
-	Roch, P., Aubert, B., 2013. French diagnostic reference levels in diagnostic radiology, computed tomography and nuclear medicine: 2004-2008 review. Radiat. Protect. Dosim. 154 (1), 52e75.
-	Romans, L. (2018). Computed Tomography for Technologists: A comprehensive text, Lippincott Williams & Wilkins.
-	Romans, L. E. (2011). "Computed Tomography for Technologists: A comprehensive Text."
-	Salama, D. H., et al. (2017). "Establishing national diagnostic reference levels (DRLs) for computed tomography in Egypt." **39**: 16-24.
-	Santos, J., Foley, S., Paulo, G., McEntee, M.F., Rainford, L., 2013. The establishment of computed tomography diagnostic reference levels in Portugal. Radiat. Protect. Dosim. 158 (3), 307–317.
-	Schindera,S.T.,Graca,P.,Patak,M.A.,Abderhalden,S.,vonAllmen,G.,Vock,P., Szucs Farkas,Z.,2009.Thoracoabdominal-aortoiliacmultidetector-row CT angiographyat 80 and 100kVp: assessment of imagequality and radiationdose. Investig.Radiol.44 (10),650–655
-	Schweitzer, M. E., Daffner, R. H., Weissman, B. N., Bennett, D. L., Blebea, J. S., Jacobson, J. A., ... & Payne, W. K. (2008). ACR appropriateness criteria® on suspected osteomyelitis in patients with diabetes mellitus. *Journal of the American College of Radiology*, *5*(8), 881-886.
-	Shrimpton, P. (2004). Assessment of patient dose in CT. EUR. European guidelines for multislice computed tomography funded by the European Commission.

-	Shrimpton, P.C., Wall, B.F., 2000. Reference doses for paediatric computed tomography. Radiat. Protect. Dosim. 90 (1–2), 249–252.
-	Siemens, A. J. E., Germany: Siemens AG. Google Scholar (2011). "Computed Tomography: Its History and Technology."
-	Tack, D., et al. (2007). Radiation dose from adult and pediatric multidetector computed tomography, Springer.
-	Tang, Y.-C., et al. (2018). "Adaptive iterative dose reduction 3D integrated with automatic tube current modulation for CT coronary artery calcium quantification: comparison to traditional filtered back projection in an anthropomorphic phantom and patients." **25**(8): 1010-1017.
-	Ulzheimer, S., et al. (2018). Multi-slice CT: current technology and future developments. Multislice CT, Springer**:** 3-34.
-	United Nations Scientific Committee on the Effects of Atomic Radiation. (2022). Sources, Effects and Risks of Ionizing Radiation, United Nations Scientific Committee on the Effects of Atomic Radiation (UNSCEAR) 2020/2021 Report: Report to the General Assembly, with Scientific Annexes.
-	Valentin, J., et al. (2007). "Published on behalf of the International Commission on Radiological Protection."
-	Van der Molen, A. J., et al. (2012). "Performance of longitudinal and volumetric tube current modulation in a 64-slice CT with different choices of acquisition and reconstruction parameters." **28**(4): 319-326.
-	Vañó, E., et al. (2017). "ICRP Publication 135: Diagnostic Reference Levels in Medical Imaging." Ann ICRP **46**(1): 1-144.
-	Varghese, B., Kandanga, I., Puthussery, P., et al., 2018. Radiation dose metrics in multidetector computed tomography examinations: a multicentre retrospective study from seven tertiary care hospitals in Kerala, South

	India. Indian J. Radiol. Imag. 28 (2), 250–257, 2018 Apr-Jun.
-	Vassileva, J. and M. J. A. J. o. R. Rehani (2015). "Diagnostic reference levels." **204**(1): W1-W3.
-	Vassileva, J., Rehani, M., Kostova-Lefterova, D., et al., 2015. A study to establish international diagnostic reference levels for paediatric computed tomography. Radiat. Protect. Dosim. 165, 70–80.
-	Verdun, F. R., et al. (2007). "CT dose optimization when changing to CT multi-detector row technology." **36**(4): 176-184.
-	Verdun, F.R., Gutierrez, D., Vader, J.P., et al., 2008. CT radiation dose in children: a survey to establish age-based diagnostic reference levels in Switzerland. Eur. Radiol. 18, 1980–1986.
-	Watson, D.J., Coakley, K.S., 2010. Paediatric CT reference doses based on weight and CT dosimetry phantom size: local experience using a 64-slice CT scanner. Pediatr. Radiol. 40, 693–703.
-	Willemink, M. J., et al. (2013). "Iterative reconstruction techniques for computed tomography Part 1: technical principles." Eur Radiol **23**(6): 1623 1631.
-	World Health Organisation (WHO), 2019. Cardiovascular diseases (CVDs). Available at: https://www.who.int/news-room/fact sheets/detail/cardiovascular-diseases-(cvds), Accessed date: 22 May 2019.
-	Yonekura, Y. (2015)."Diagnostic Reference Levels Based on Latest Surveys in Japan." Available at: http://www.radher.jp/J RIME/report/DRLhoukokusyoEng.pdf , Accessed date: 22 May 2019
-	Zamora, D., Kanal, K., Dickinson, R., Shuman, W., & Stewart, B. (2012). TU-G-217BCD-09: Integration of Recent NEMA (MITA) XR-25 CT Dose-Check Standard into Clinical Practice. *Medical Physics*, *39*(6Part25), 3926-3926

-	Zhang, L., et al. (2019). "The impact of adaptive iterative dose reduction 3D on the improvement of shoulder image quality in head and neck CTA." **35**(5): 887-891.

APPENDIX

Appendix (1)

Technical specification of CT scanner

Hospital: ……..……

Scanner type (manufacture): ……

Scanner model : ……...

Detector type: …….

Year of installation: ……...

Appendix (2)

Work Sheet

Subject No. …… Gender: …… Hospital : ……..……

Age (year): …… weight (Kg) : …….. Height (cm) : ……..

Clinical Indication: ……..

parameter	Value	parameter	Value
Tube potential (KVp)		CTDIvol (mGy)	
mAs		DLP single (mGy.cm)	
Scan length		DLP total (mGy.cm)	
Pitch		No. of phase	
Slice thickness (mm)		Total slice No.	

Contrast Media:

Administration	Type of CM	Volume of CM	Concentration of CM Mgl/mL	Injection rate mL/s
Oral				
Intravascular				